

Copyright
by
Mark Jacob Goldman
2013

Nitrosamine Formation in Carbon Capture

APPROVED BY

SUPERVISING COMMITTEE:

Gary Rochelle, Supervisor

Leah Hildebrandt

Nitrosamine Formation in Carbon Capture

by

Mark Jacob Goldman

THESIS

Presented to the Faculty of the McKetta Department of Chemical
Engineering

The University of Texas at Austin

in Partial Fulfillment
of the Requirements

for

Engineering Honors

THE UNIVERSITY OF TEXAS AT AUSTIN

May 2013

Dedicated to my parents who have consistently given me freedom,
opportunity, and support throughout my life.

Acknowledgments

Many people helped me in this thesis, and without them this work would not be possible. Nathan Fine taught me most of the methods used, supported me throughout the processes, and provided critical insight necessary for this work. Without him, this work would not be possible. Dr. Gary Rochelle has also given countless hours providing valuable insight on my experimental design and analysis methods. He also worked significantly to secure the funding that was essential for this work to take place. Dr. Leah Hildebrandt assisted me greatly with the third chapter along with sharing advice for my future career, and I am very appreciative of her.

Dr. Grant Willson, Dr. Eric Anslyn, and Dr. Thomas Edison helped me to better understand concepts that I had little previous exposure to. Omakar Namjoshi recommended studying methylethanol amine which enabled me to better understand function dependence on reaction rate. Dr. Alexander Voice developed the analytical methods for the analysis. In addition, my friends and family were indirectly invaluable for supporting me through this process. Last, I would like to thank the Texas Carbon Management Program supporters for funding this research.

Nitrosamine Formation in Carbon Capture

Mark Jacob Goldman, B.S.
The University of Texas at Austin, 2013

Supervisor: Gary Rochelle

Carbon capture using amine scrubbing is an effective way to reduce CO₂ emissions, but nitrosamines, a class of carcinogenic compounds, form from nitrogen oxides (NO_x) in the process. Kinetic analysis of reactions involving nitrite and ethanol amine (MEA), piperazine (PZ), diethanol amine (DEA), methylethanol amine (MMEA), and methyldiethanol amine (MDEA) determined the reaction rate of each amine under various conditions. The reactions involving MEA, PZ, DEA, and MMEA were first order in nitrite, carbamate species, and hydronium ion. The tertiary amine, MDEA, did not fit the same rate law. A model accurately predicts reaction kinetics for unhindered primary and secondary amines. The rates of reaction revealed that primary amines react approximately 10 times slower than secondary amines under identical reaction conditions. Increased reactivity was noted in secondary amines which have more electron withdrawing groups attached to the amine. Two proposed mechanisms involve protonation of the carbamate species, nucleophilic attack

of carbamic acid by nitrite, and formation of bicarbonate and a nitrosamine. The comparative kinetics can be applied to the analysis of the steady state concentration of nitrosamines in carbon capture, can help identify inhibitors for this reaction, and can be applied to the use of blends to mitigate nitrosation.

Table of Contents

Acknowledgments	v
Abstract	vi
List of Tables	x
List of Figures	xi
Chapter 1. Introduction	1
1.1 History of Carbon Capture	1
1.2 Mechanics of Carbon Capture	2
1.3 Solvent Management Issues	4
1.4 Relevant Amines	5
1.4.1 Piperazine	6
1.4.2 Monoethanol Amine	7
1.4.3 Diethanol Amine	8
1.4.4 Methyldiethanol Amine	8
1.4.5 Methylethanol Amine	8
1.5 Amine Reaction with Nitrite	9
1.5.1 Primary Amines	10
1.5.2 Secondary Amines	10
1.5.3 Tertiary Amines	11
Chapter 2. Methods	13
2.1 Safety Considerations	13
2.2 Experimental Runs	13
2.3 pH Measurement	15
2.3.1 Ionic Strength	15
2.3.2 Method Development	15

2.3.3	Final Method	18
2.4	Nitrite Standards	19
2.4.1	Standard Preparation	19
2.4.2	Standard Results	20
2.5	Other Solution Analysis	22
2.6	Calculations for Analysis	23
2.6.1	Rate Regression	23
2.6.2	Predicting pK_a at Elevated Temperatures	23
2.6.3	Predicting pH in Amine-CO ₂ Solutions	25
Chapter 3.	Model Development	26
3.1	Nitrite Dependence	28
3.2	pH Dependence	29
3.3	Carbamate Dependence	31
3.4	Temperature Dependence	35
3.5	Kinetic Model	35
Chapter 4.	Amine Comparison	39
4.1	Nitrite Consumption in Primary Amines	39
4.2	Nitrosamine Formation in Tertiary Amines	42
4.3	Nitrosamine Formation in Secondary Amines	45
4.3.1	Diethanol Amine	45
4.3.2	Methylethanol Amine	47
4.4	Rate Comparison	49
4.4.1	Activation Energy and Preexponential Factor	49
4.4.2	Formation Rates at Conditions	49
4.5	Reaction Mechanism	53
4.6	Broader Impact	55
Vita		62

List of Tables

2.1	Chemical purities and sources	14
2.2	Anion chromatography calibrations	21
2.3	pK_a and ΔH of amines	24
3.1	Summary of piperazine experiments	27
3.2	Carbamate dependence	33

List of Figures

1.1	Carbon capture system	3
1.2	Carbamate formation reaction	3
1.3	Bicarbonate formation reaction	4
1.4	Carcinogenicity of nitrosamines in CO ₂ capture	5
1.5	Amine structures	6
1.6	Nitrosamine formation reaction	9
1.7	Degradation of primary nitrosamines	10
1.8	Literature mechanism for nitrosation	11
2.1	pH dilution affect	16
2.2	pH method comparison	18
2.3	Nitrite standard comparison	20
2.4	Nitrite regression method	24
3.1	Rate dependence on nitrite	28
3.2	Rate dependence on pH	30
3.3	Rate dependence on CO ₂	34
3.4	Rate dependence on Temperature	36
3.5	PZ model performance	37
4.1	MEA nitrosation rate	41
4.2	MDEA experimental results	43
4.3	DEA nitrosation rate	46
4.4	MMEA nitrosation rate	48
4.5	Comparison of activation energy	50
4.6	Comparison of preexponential factors	51
4.7	Comparison of k ₁ using natural solution pH	52
4.8	Mechanism without nitrosonium ion formation	53
4.9	Mechanism with nitrosonium ion formation	54

Chapter 1

Introduction

1.1 History of Carbon Capture

The human population is largely dependent on fossil fuels for energy. The primary product of fossil fuel combustion is carbon dioxide (CO_2). CO_2 in the atmosphere can absorb infrared radiation leaving earth's surface and re-emit it back towards earth. This behavior classifies CO_2 as a green house gas, and its presence warms the earth.

Due to the strong dependence on fossil fuel combustion for energy and the effect of global warming from fossil fuel combustion, a large movement has grown to prevent CO_2 from escaping into the atmosphere. This process involves carbon capture, isolating CO_2 post-combustion, and carbon sequestration, storing CO_2 to prevent the greenhouse effect.

One of the most effective locations to capture CO_2 is at large power plants due to the scale of carbon emissions. At these locations, capture equipment can be installed to reduce CO_2 emissions by 90%. One efficient capture technology uses amine scrubbing to isolate CO_2 .^[19] This thesis discusses one of the issues involved with this system.

1.2 Mechanics of Carbon Capture

The basic carbon capture system involves an absorber, stripper, and heat exchanger. Amine solvents with low CO_2 concentrations flow down the absorber and counter-currently encounters the exit gas from a power plant. During this phase, CO_2 transfers into the amine solution. The amine solution exiting the absorber then enters a heat exchanger where it is heated by the hot solution exiting the stripper. This temperature increase decreases the solubility of CO_2 in the solution, so the pressure increases.

The heated solution then enters the stripper where the solution is further heated and releases CO_2 . The hot solution is then cooled by the solution exiting the absorber and reenters the absorber. This cycle continues to regenerate the solvent and extract CO_2 . Figure 1.1 shows this process schematic.

Amines chemically absorb CO_2 in two main mechanisms. The first, shown in Figure 1.2 involves a reaction between the two amines and CO_2 to form a carbamate compound and a protonated amine. This reaction consumes two amine groups. The second reaction, in Figure 1.3, involves the protonation of an amine and the formation of bicarbonate.

The rate of the reaction that forms carbamate dominates for unhindered primary and secondary amines. Tertiary amines cannot form the carbamate compound without having an unstable positive charge, so the formation of bicarbonate dominates. Mixing primary or secondary amines with tertiary amines enables the formation of carbamate with the accepted proton falling

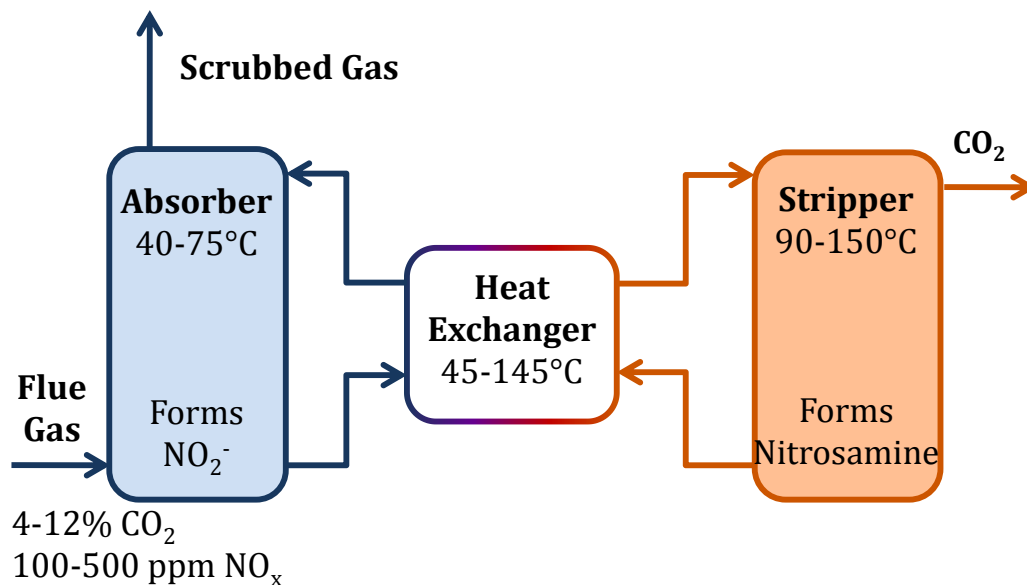


Figure 1.1: The carbon capture system isolates CO₂ from the flue gas of power plants using an absorber, stripper, and heat exchanger.

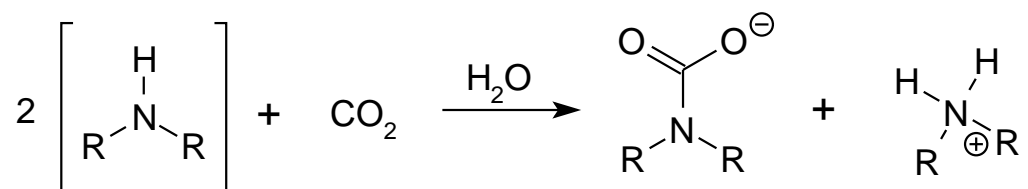


Figure 1.2: This general reaction depicts the formation of carbamate compounds and protonated amines from unhindered primary and secondary amines and CO₂.

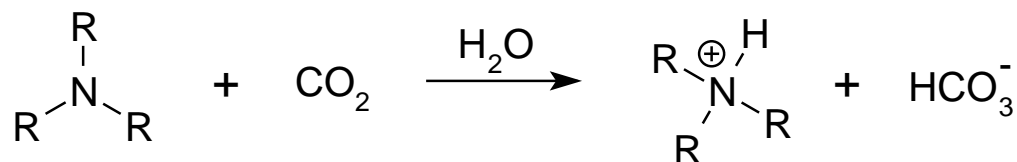


Figure 1.3: This general reaction depicts the formation of protonated amines and bicarbonate from hindered primary/secondary amines or any tertiary amines with CO_2 .

on the tertiary amine.

1.3 Solvent Management Issues

The amines solutions undergo degradation during use. This can physically be seen as the initial solvent put into the reactor turns opaque after use. Degradation occurs oxidatively and thermally. Oxygen present in the flue gas will oxidize the amines. Significant work has been conducted to study how oxidative degradation affect the solvent performance.[11] Thermal degradation occurs when amines undergo reactions at the high temperatures of the stripper. Both of these mechanisms can change the physical properties of the solvent and lower solvent performance.

Another issue in solvent management involves the formation of carcinogenic compounds called nitrosamines. Figure 1.4 displays the toxic doses of two nitrosamines in carbon capture along with that of benzene and ethanol. These compounds have the $\text{N}=\text{N}-\text{O}$ functional group and form from the introduction of NO_x gas. NO_x gas is present in the flue gas and will react with

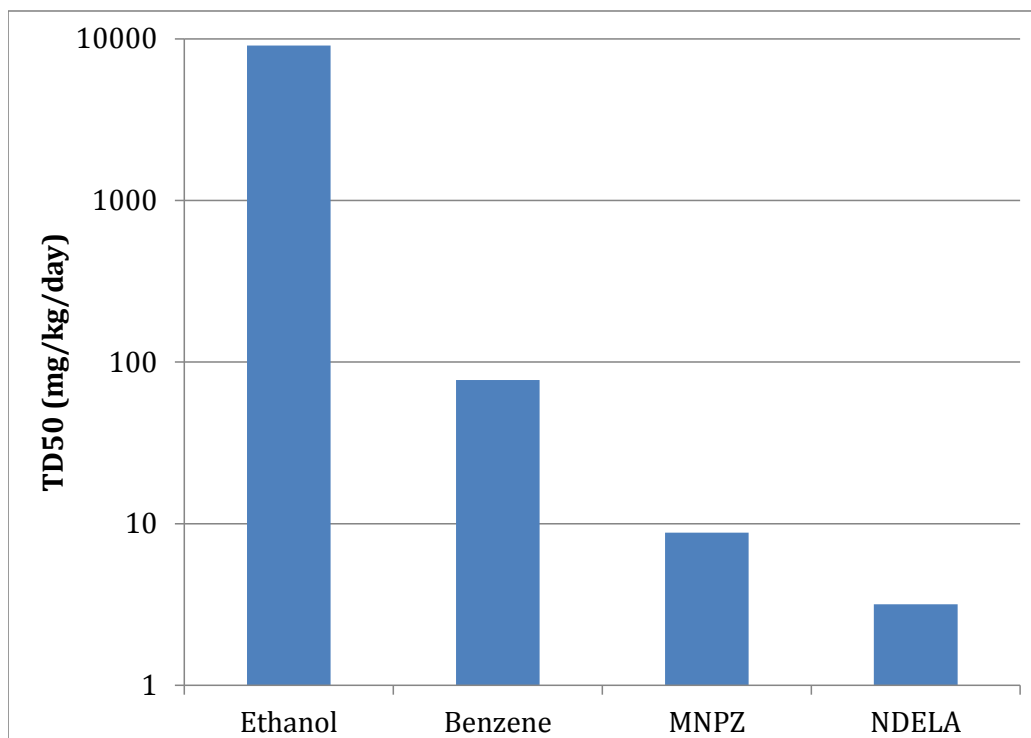


Figure 1.4: The carcinogenicity in rodents of mononitrosopiperazine (MNPZ) and nitrosodiethanol amine (NDELA) are shown against that of benzene and ethanol. The toxic dose (TD50) represents the daily dose required to cause cancerous tumors in 50% in the test animals. A smaller TD50 represents higher potency.

the solution to produce nitrite ions (NO_2^-). Alternatively, the NO_x gas can also react with the solution directly to form nitrosamines.[6]

1.4 Relevant Amines

Various amines are used in carbon capture. Monoethanol amine (MEA) is the current standard for carbon capture in natural gas treating. Piperazine

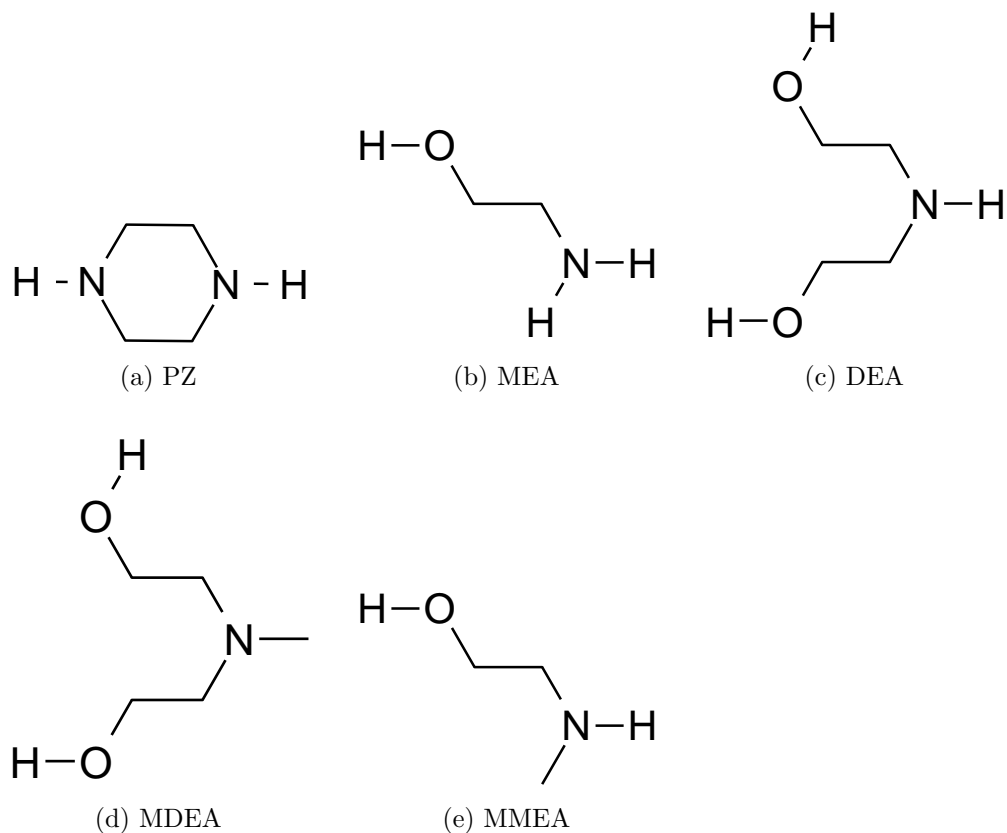


Figure 1.5: Structures of amines studied

(PZ) absorbs CO_2 faster than MEA, and current research is helping build a case for usage of PZ in amine scrubbing. The amines structures appear in Figure 1.5 along with other amines studied.

1.4.1 Piperazine

Piperazine (PZ) is a 6 membered cyclic diamine. Though it is not the standard amine for CO_2 capture, PZ has many positive attributes. Due to

PZ's low volatility, less amine escapes into the environment. It has high thermal stability up to 150°C, so higher CO₂ pressures can occur in the stripper without significant degradation of PZ. It's high heat of absorption of CO₂ also helps produce high stripper pressures. PZ also has a high CO₂ capacity because there are two amine groups in each molecule.[19]

One drawback on PZ involves it's solubility. Concentrated solutions of 8 molal PZ in pure water results in the formation of Piperazine-hexahydrate solid at room temperature. Heating to 40°C or absorbing CO₂ will dissolve the complex. Because of this issue, PZ cannot be used with minute amounts of CO₂. PZ also exhibits a solubility limit when the moles of CO₂ approaches the moles of PZ. The solubility of this complex does not have a strong temperature dependence due to a low heat of dissolution, so heating will not improve solubility.

The solubility drawbacks of PZ lead it to be mixed with other amines for usage in carbon capture. With these mixtures, greater solubility can be obtained.

1.4.2 Monoethanol Amine

Monoethanol amine (MEA) is currently the standard amine for usage in carbon capture systems. This amine is cheaper to produce when compared to PZ, but has higher volatility and degradation rates. MEA does not form solids in solution, so solubility limits are not of concern.

1.4.3 Diethanol Amine

Diethanol amine (DEA) is essentially MEA with another ethanol group attached to the nitrogen. This significantly changes the reaction chemistry, and gives DEA a lower pK_a than MEA. DEA normally occurs in CO₂ capture system as a byproduct of MEA production, so using MEA will introduce DEA into the system.

1.4.4 Methyldiethanol Amine

Methyldiethanol amine (MDEA) has been studied in blends with PZ to improve solubility issues of PZ with minimal loss of performance. It is also currently used in SO_x scrubbing systems. Since it is a tertiary amine, it cannot form a carbamate complex. Instead, MDEA acts as a proton acceptor to give bicarbonate. This reaction is slower than the carbamate formation, so MDEA is sought as an additive in a blend instead of an isolated solvent.

1.4.5 Methylethanol Amine

Methylethanol Amine (MMEA) is an amine that is not currently used in carbon capture. However, studying the reaction rate of MMEA highlights the structure relationship between electron withdrawing groups on nitrosation rates. DEA has more electron withdrawing groups than MMEA, so comparing MMEA to DEA can improve understanding about the importance of electrons on the amine group.

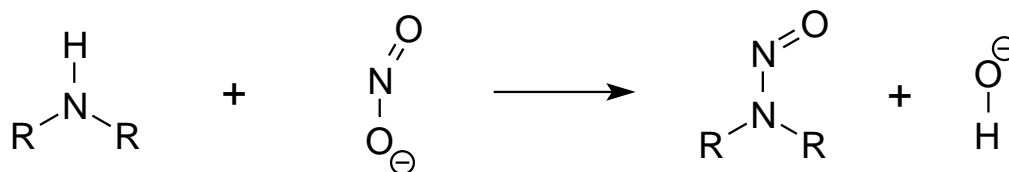


Figure 1.6: This general reaction of nitrite with a primary or secondary amine forms a nitrosamine compound

1.5 Amine Reaction with Nitrite

Amines react with nitrite to form carcinogenic nitrosamines described previously in section 1.3. An overall reaction is shown in Figure 1.6.

Figure 1.6 indicates that the reaction of interest produces a base. Under carbon capture conditions, bicarbonate is normally produced. Due to the buffered solvent and the low concentration of nitrite, the pH change due to this reaction would be negligible.

Kinetics of nitrosation have been studied extensively under acidic conditions because much nitrosamine formation was thought to form inside human stomachs from nitrite-treated meat. This research concluded that the di-protonated form of nitrite was the nitrosating agent causing nitrosamine formation.[7] This active species definitely required a strongly acidic environment since the pK_a of nitric acid is less than 4.[7] However, less research of nitrosation has been conducted under basic conditions, especially in the presence of CO_2 .

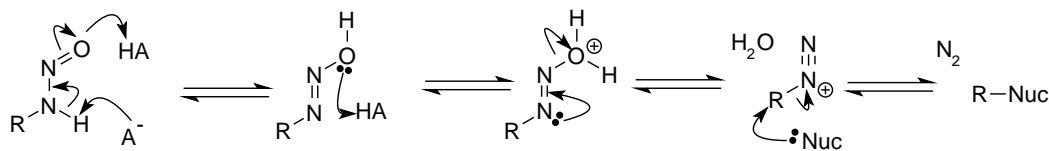


Figure 1.7: Nitrosamines formed from primary amines undergo degradation through proton transfer from the nitrogen and α carbon to the oxygen resulting in the loss of water. Finally, nitrogen gas escapes the system leaving either a secondary amine, alcohol or other product.[7]

1.5.1 Primary Amines

Primary amines, like MEA, form nitrosamines under the general reaction shown by Figure 1.6, but these nitrosamines are not very stable. At the temperatures of the stripper, nitrosamines which formed from primary amines will quickly degrade into nitrogen gas and other products through the mechanism shown in Figure 1.7.[7]

1.5.2 Secondary Amines

Like primary amines, secondary amines form nitrosamines as shown in Figure 1.6. However, since the secondary nitrosamines do not have a hydrogen attached to the nitrogen group, they are unable to undergo the fast degradation mechanism shown in Figure 1.7. Work is currently being done to characterize how secondary nitrosamines degrade in carbon capture solvents.[8] From this work, it is evident that higher temperatures are required for degradation of nitrosamines than their formation.

In 2010, N-nitrosopiperazine (MNPZ), a carcinogenic nitrosamine formed

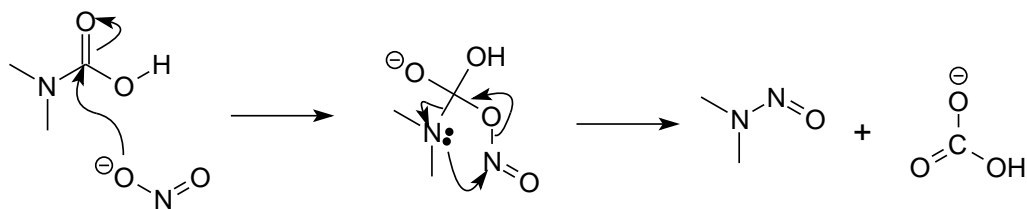


Figure 1.8: The mechanism proposed by Sun and Lv for nitrosation of dimethylamine which uses CO_2 as a catalyst. CO_2 forms the carbamate ion with the amine, turns into carbamic acid, and then reacts with nitrite.[22, 17]

from PZ, was found in CO_2 capture pilot plants running PZ solvent.[15] Researchers initially used theoretical methods to better understand how this reaction could proceed under basic conditions. One hypothesis discussed in two papers involved using CO_2 as a catalyst. These researchers mentioned the mechanism shown in Figure 1.8 as a potential reaction pathway with an activation energy of 45 kcal/mol.[22, 17]

1.5.3 Tertiary Amines

Tertiary amines are unable to form stable nitrosamines directly since the central nitrogen would result with a formal charge of +1. For nitrosation to proceed with tertiary amines under acidic conditions, one of the alkyl substituents must be removed from the amine. The kinetics for this reaction under acidic conditions indicate that tertiary amines nitrosate 10,000 times slower than secondary amines.[7]. The kinetic study also suggests that an aldehyde product would form from the dealkylation. Even with this knowledge, the mechanism for nitrosation has not been studied under basic conditions char-

acteristic of carbon capture.

If the reaction mechanism for nitrosation under acidic conditions is similar to basic conditions, tertiary amines need to convert to a secondary amines before forming a nitrosamine. In carbon capture, this can happen two ways: oxidative and thermal degradation.

Chapter 2

Methods

2.1 Safety Considerations

As mentioned in section 1.3, nitrosamines are carcinogenic. Certain safety measures were taken into account to reduce exposure to nitrosamines. Solutions were heated inside convection ovens connected to fume vents. Nitrosamine samples were contained inside a single fume hood. In addition to these measures, gloves, goggles, and lab coats were worn whenever inside the laboratory.

2.2 Experimental Runs

To determine the rate of nitrosamine formation, a solution needs to be heated for different lengths of time and analyzed to see how the concentration varies with time. Solutions were placed inside 3/8 inch stainless steel tubing with Swagelok cap, known as Swagelok cylinders. These give a constant volume container that can withstand high pressures at nitrosation temperatures.

For each solution and temperature, five Swagelok cylinders were heated with the same solution inside. The cylinders were removed over an arithmetic time scale to correspond with approximately 50% to 95% completion of the

Table 2.1: Sources of chemicals and purity used in the experiments.

compound	purity	source
CO ₂	99.5%	Matheson Tri-Gas
DEA	99%	Acros Organics
KHCO ₃	99.5%	Sigma
KOH	87%	Fischer Scientific
MEA	98.5%	Eastman Chemical
MMEA	99%	Acros Organics
MDEA	99%	Acros Organics
MNPZ	98%	Toronto Research Chemicals
NaNO ₂	98.5%	Acros Organics
PZ	99%	Sigma-Aldrich

reaction. When using the convection ovens, the first sample was not removed after less than an hour because significant time is necessary heat up the cylinders to the oven temperature.

The samples were removed from the cylinders and placed into 15 mL amber vials since nitrosamines degrade by UV light.[20] The samples were then diluted between 30× to 50× into 2 mL amber vials. The magnitude of dilution depended primarily on the concentration of the original sample.

The samples were analyzed using High Pressure Liquid Chromatography or an chromatography instrument. Both instruments produced graphs with peaks corresponding to nitrite. Using the nitrite calibration curves discussed in section 2.4 and the magnitude of dilution, the concentration of nitrite in each sample was found.

2.3 pH Measurement

Since preliminary results indicated that solvent pH strongly affects nitrosamine formation in PZ, it became necessary to measure pH accurately for each solution analyzed. To do this, the pH probe from an automatic titrator, described in section 2.5, measured the pH. This device had inaccuracies from its calibration to dilute solutions and the inability to measure temperature.

2.3.1 Ionic Strength

Since the pH probe was calibrated for dilute solutions, our procedure involved diluting samples before any pH measurement. Diluting samples lowers the ionic strength. Since equilibrium constants for acid/base reactions are dependent on ionic strength, inaccuracies result from diluting. In an attempt to correct for this error, a series of dilutions were measured in the device as shown in Figure 2.1.

Increasing dilutions decreases the measured pH value because ionic strength stabilizes ions by decreasing their activity coefficient. With dilutions, the activity of protonated amines decreases less than other species, so equilibrium is driven towards unprotonated amines and hydronium ions. This results in a lower pH.

2.3.2 Method Development

Different methods were developed to account for the shift in pH shown in Figure 2.1. We used the four DEA solutions from subsection 4.3.1 to mea-

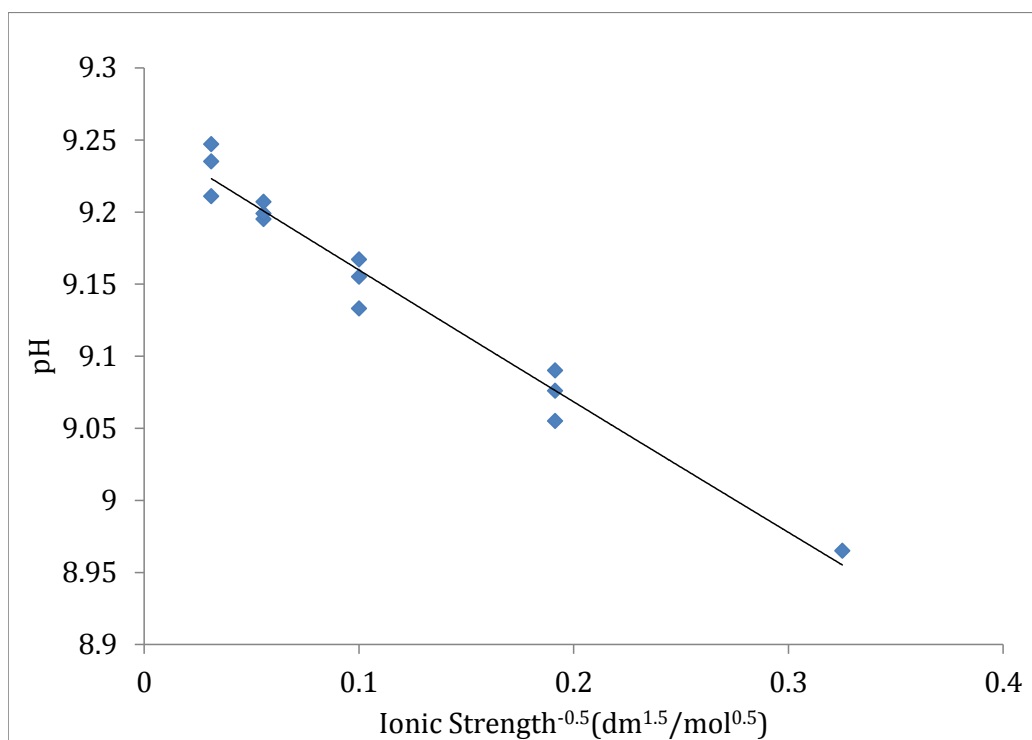


Figure 2.1: Data were from a solution of 8 molal PZ loaded to 0.3 mol CO₂/mol nitrogen. The regressed line shows the expected effect of the Debye-Hückle theory.

sure pH in different ways. After each pH method was tried, the data was regressed with reaction rates to see if a better correlation resulted. The best correlation would correspond with the most accurate pH measurements.

The first method attempted to extrapolate a line from the Debye-Hückle theory shown in Figure 2.1. Each DEA solution was diluted at three points over an order of magnitude. Each solution was regressed independently to find the dependence of the solution pH on ionic strength. The high loading experiments showed an opposite dependence than the low loading experiments. This was most likely due to the formation of bicarbonate. The resulting data was extrapolated to find the concentrated solution pH. When applied to the experimental rates, a correlation coefficient of 0.90 resulted.

The second method involved measuring the concentrated solution. Problems with this method include a large amount of sample (4 mL) required to immerse pH probe and the dilute calibration of the pH probe. The first sample tested took over 50 minutes to converge on a pH reading and drifted 0.012 during the last 30 minutes. Subsequent measurements took approximately 5 minutes to reach a final value. The difference in timing likely resulted from a change in concentration inside the pH probe increasing error in this method. The pH values were correlated with the reaction rates yielding a correlation coefficient of 0.89.

The best method utilized involved measuring all four solutions at $300\times$ dilutions, and ignoring ionic strength affects. When correlated with reaction rates, a correlation coefficient of 0.97 was obtained. However, this method

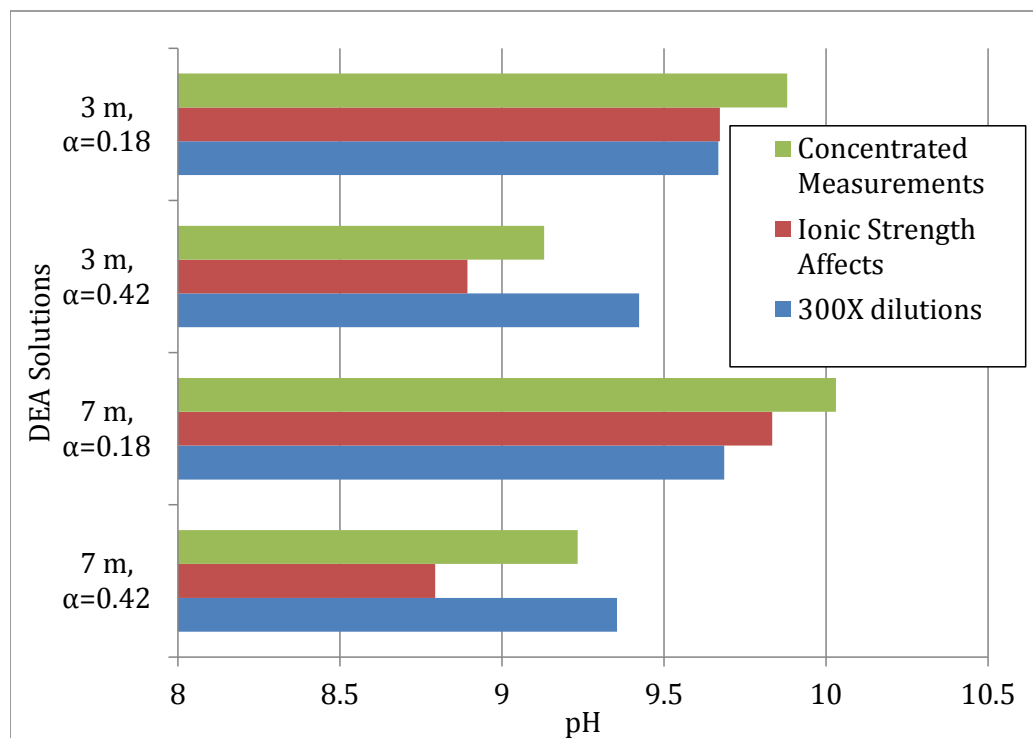


Figure 2.2: The values of pH for all three methods. The concentrated measurements correlated least with the data while the 300 \times dilutions showed the best correlation.

contains some unregressed systematic error from ionic strength affects. The pH readings of all three methods are shown in Figure 2.2.

2.3.3 Final Method

The final method developed for measuring the pH involves diluting samples so that the amine concentration loosely correlates with a three hundred dilution of PZ. Each diluted sample is stirred for five minutes with the pH probe in the solution. Stirring is stopped, and the measured if the measured

pH value stabilized for twenty seconds, it is recorded, if it is not stable, more stirring is conducted till the pH is stable. After each pH measurement, the sample is stirred for one minute. Then the stirring is stopped so another pH measurement can be taken. This process is repeated till three measurements are taken. If the measurements show drift, more measurements are taken till the most recent samples are within 0.002 units. The average is then taken of the measurements.

2.4 Nitrite Standards

To convert the peak areas obtained from the HPLC and Anion chromatography into concentrations, a correlation between peak areas and known concentrations is necessary. This is obtained by making a series of dilutions of a known concentration. A linear relationship describes peak areas and concentration for dilute solutions. However, since less dilute solutions impact linear regressions more than more dilute solutions, large errors will result in dilute solutions if all points are regressed together.

2.4.1 Standard Preparation

To prepare standards, a 500 ppm solution was prepared by adding 0.1 g of a pure component (taking into account purity and spectator ions) into 200 mL of water. The mixture was stirred till well mixed. Dilutions from 5× to about 200× were taken. If lower calibrations are necessary, a dilution of the stock solution can be made to enable further dilution. This should result

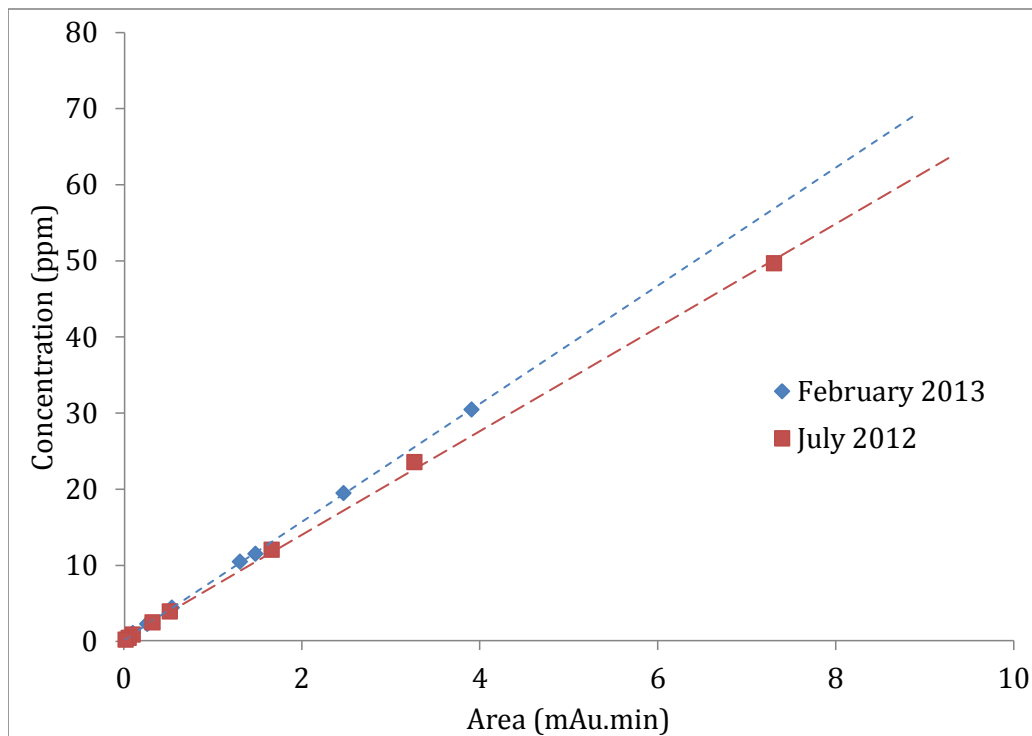


Figure 2.3: Two nitrite standards for the anion chromatography instrument appear above. The more recent standard has a slightly higher slope than the older standard.

in concentrations ranging from 0.5 to 100 ppm.

2.4.2 Standard Results

The anion chromatography instrument was calibrated for nitrite during July 2012 and February 2013. The two calibrations are shown in Figure 2.3.

The result from Figure 2.3 may indicate a degraded column, but since multiple standards have not been conducted at one time, there is no knowledge of the uncertainty of the standard-making method, so no conclusive knowledge

Table 2.2: Calibration curves for nitrite in the anion chromatography equipment based from two separate calibrations.

calibration date	ppm range	m	b	r^2
July 2012	1-50	6.78 ± 0.09	0.59 ± 0.29	0.9993
July 2012	0.1-2.5	7.57 ± 0.16	0.06 ± 0.024	0.9987
February 2013	2-30	7.74 ± 0.04	0.25 ± 0.09	0.9998
February 2013	0.3-2	8.31 ± 0.61	0.13 ± 0.09	0.9894

about the degradation of the column can be determined from just these two standards.

The equations for each standard follow the form:

$$C = m \times A + b \quad (2.1)$$

Where C is concentration in ppm and A is area in milli-absorbance unit \times minute.

The standard errors shown in Table 2.2 indicate that the slope difference does not result from inaccuracies during dilution. The difference in slope indicates a change in instrument performance. In particular, the poor r^2 value for the later dilute standard indicates an increase in the minimum detection limit. Other errors in this standard can be created by initial measurement of the stock solution.

2.5 Other Solution Analysis

Methods were used to obtain the amine concentration and total inorganic CO₂ added to the system. The amine concentration involves a Metrohm Titrando 835. Sulfuric acid at 0.1 M is added to a diluted solution sample using an automatic titrator. A computer plots the pH as a function of amount of acid added and determines the equivalence point. The final equivalence point represents when all the amine has been protonated. The amount of acid needed corresponds to the gravimetric concentration of amine according to Equation 2.2.

$$C_{amine} = \frac{V_{acid}M_{acid}}{m_{solution}} \quad (2.2)$$

The total inorganic carbon method determined the amount of carbamate, bicarbonate, carbonate, carbonic acid, and free CO₂ in the solution. To do this, a sample of solution, which is usually diluted one hundred times, is injected into a solution of phosphoric acid. All the carbonate and carbamate species are converted into free CO₂ which is then carried by N₂ gas into a CO₂ analyzer. Because the flowrate and temperature of the carrier gas may change, standards were taken after each sample run using an inorganic carbon standard from Ricca Chemical Company. To improve precision, triplicate measurements of each sample were taken. More information about the titration and total inorganic carbon method can be found in Freeman's dissertation.[11]

2.6 Calculations for Analysis

Determining reaction kinetics from the experimental data required theory-based calculations. These enabled the reaction conditions at elevated temperatures and the pH of an unknown amine with CO₂ to be estimated. It also allowed for rate constants to be derived for each time series.

2.6.1 Rate Regression

Nitrosamine formation is first order in nitrite.[13] To discover the pseudo first order rate constant, k_{obs} , the natural log of nitrite concentration for the five samples was plotted against time (shown in Figure 2.4). The opposite sign of the slope represents k_{obs} .

$$\frac{d[NO_2^-]}{dt} = k_{obs}[NO_2^-] \quad (2.3)$$

2.6.2 Predicting pK_a at Elevated Temperatures

The pK_a of amines changes with temperature according to van't Hoff equation.[1] This equation requires a pK_a at a reference condition and an enthalpy of disassociation which were found from literature. For amine solutions with CO₂, the protonated amine and unprotonated amine buffer the solution. The pK_a change of the amine over the temperature range directly correlates with the pH change of the solution measured at room temperature.

The solutions of PZ that were not conducted in a buffer used the Inde-

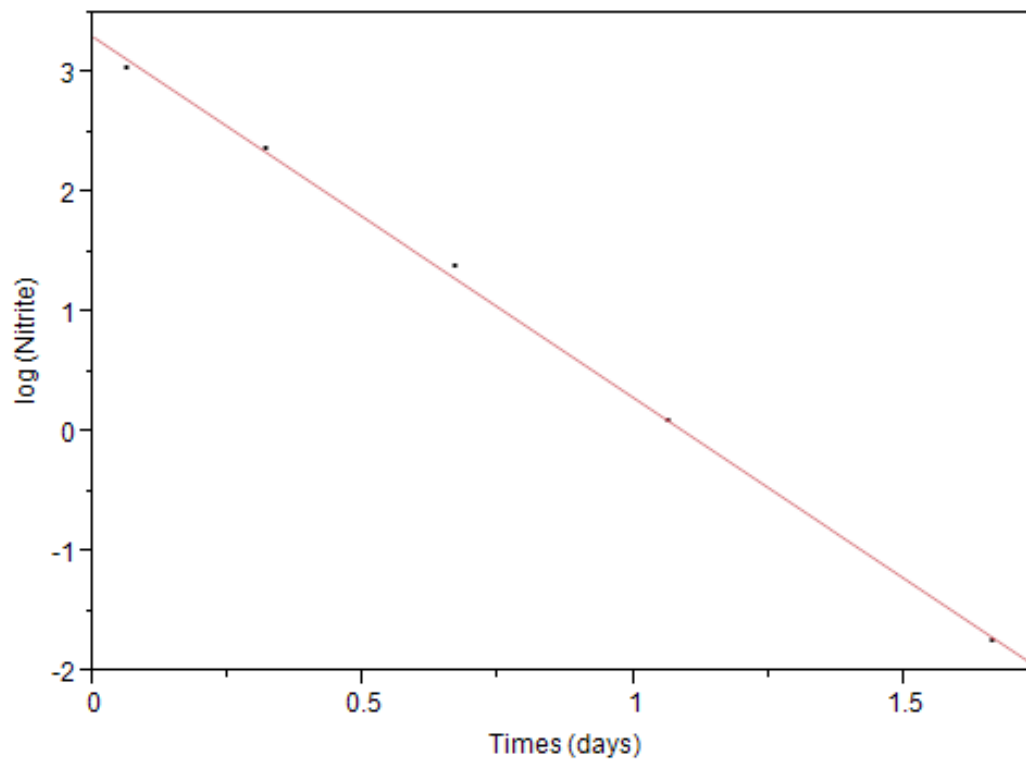


Figure 2.4: k_{obs} was found using a linear regression on statistical software. This plot shows nitrite disappearance in 3 molal MEA loaded to 0.15 mol CO₂ / mol N.

Table 2.3: pK_a and enthalpy of disassociation for amines used in estimating pH change with temperature.

Amine	pK_a at STP	ΔH (kJ/mol)	source
MEA	9.498	50.52	[12]
PZ	9.731	42.89	[12]
DEA	8.883	42.08	[12]
MMEA	9.85	44.4	[14]
MDEA	9.498	50.52	[16]

pendence model to predict nitrosation rates.[10] All other solutions and amines utilized the method in this section.

2.6.3 Predicting pH in Amine-CO₂ Solutions

Solutions of amines have various pH values at different temperatures. Extensive models have been derived PZ and MEA.[10] However, models for each potential amine cannot reasonably be developed, so a method for predicting pH of loaded solutions is necessary. One quick way to estimate the pH of solutions of various amines with loaded CO₂ only requires the pK_a at standard conditions, the standard enthalpy of disassociation, and the loading.

Using the Henderson-Hasselbalch equation and equations shown in Figure 1.2 and Figure 1.3, an estimation of the pH of a solution can be estimated for loadings between 0.1 and 0.4 mol CO₂/mol amine group.

$$pH = pK_a + \log\left(\frac{\alpha}{1 - 2\alpha}\right) \quad (2.4)$$

$$pH = pK_a + \log\left(\frac{\alpha}{1 - \alpha}\right) \quad (2.5)$$

Equation 2.4 shows the pH prediction for carbamate forming amines, and Equation 2.5 shows the pH prediction for sterically hindered and tertiary amines. α represents the loading in units of mol CO₂/mole amine group.

Chapter 3

Model Development

PZ was used for to develop the nitrosation model since most previous work involved PZ characterization. The experimental set of data is shown by Table 3.1. The rate is reported as k_{obs} estimated from the data from each experiment by Equation 3.1. This value is compared to the k_{obs} estimated by a global correlation using Equation 3.5. A significant rate of nitrite disappearance was observed in 0.5-5 mol/dm³ PZ at 50-100°C. The rate was also measured in phosphate buffered solution at 135°C at 0.1 mol/dm³ PZ.

The yield of N-nitrosopiperazine (MNPZ) is defined as the final MNPZ over the difference in the final and initial nitrite. An average yield of $95 \pm 11\%$ was obtained for the 14 experiments discussed here. The high yield indicates no major competing reactions consuming nitrite occur in the PZ solvent. This value is slightly below unity because MNPZ decomposes at these reaction conditions.[8]

Small, but quantifiable, amounts of N, N'-dinitrosopiperazine (DNPZ) were found in various samples. However, the nitrite yield to DNPZ was less than 1% under these conditions, so it is not a major product.[8]

Table 3.1: Summary of PZ experiments. Between 6 and 10 mmol NaNO₂ per mol PZ was added to each sample. Total CO₂ represents both physically and chemically absorbed CO₂. k_{obs} is the observed first order rate constant for nitrite disappearance from each experiment. Yield describes how much nitrite formed MNPZ.

Temp (K)	PZ (M)	pH (at T_{rxn})	Total CO ₂ (M)	k_{obs} (s ⁻¹ × 10 ⁶)		Yield (%)
				Exp.	Model	
135	0.099 ± 0.004	7.85 ± 0.01 ^a	0.040 ± 0.003	52 ± 6	44 ± 12	86
135	0.099 ± 0.004	7.37 ± 0.01 ^a	0.040 ± 0.003	120 ± 10	133 ± 36	112
135	0.099 ± 0.004	7.58 ± 0.01 ^a	0.040 ± 0.003	72 ± 4	81 ± 22	105
135	0.099 ± 0.004	8.04 ± 0.01 ^a	0.040 ± 0.003	30 ± 2	28 ± 8	112
100	5.0 ± 0.2	9.09 ± 0.05 ^b	1.00 ± 0.08	6.3 ± 0.2	6.9 ± 2.2	96
100	5.0 ± 0.2	8.72 ± 0.05 ^b	2.13 ± 0.17	32 ± 1	35 ± 11	81
100	5.0 ± 0.2	8.36 ± 0.05 ^b	2.94 ± 0.24	112 ± 4	111 ± 35	80
100	5.0 ± 0.2	7.69 ± 0.05 ^b	4.14 ± 0.33	675 ± 26	733 ± 229	100
100	4.9 ± 0.2	8.30 ± 0.05 ^b	3.05 ± 0.24	149 ± 3	132 ± 41	101
100	1.7 ± 0.1	8.22 ± 0.05 ^b	1.07 ± 0.09	70 ± 3	56 ± 18	97
100	.48 ± 0.02	8.18 ± 0.05 ^b	0.30 ± 0.02	13.7 ± 0.2	17 ± 5	94
100	4.29 ± 0.04	8.24 ± 0.01 ^c	0.011 ± 0.001	3.2 ± 0.1	0.5 ± 0.1	82
80	5.0 ± 0.2	8.61 ± 0.05 ^b	2.96 ± 0.24	13.3 ± 0.3	15 ± 4	76
50	5.0 ± 0.2	9.08 ± 0.05 ^b	2.96 ± 0.24	0.43 ± 0.01	0.4 ± 0.1	99

^aBuffered by 0.5 M phosphate adjusted by KOH. pH measured at room temperature and corrected to reaction temperature

^bpH at reaction temperature estimated by 'Independence' in Aspen Plus

^cIncluded 2.5 M H₂SO₄, pH measured at room temperature and adjusted to reaction temperature, not regressed in the model

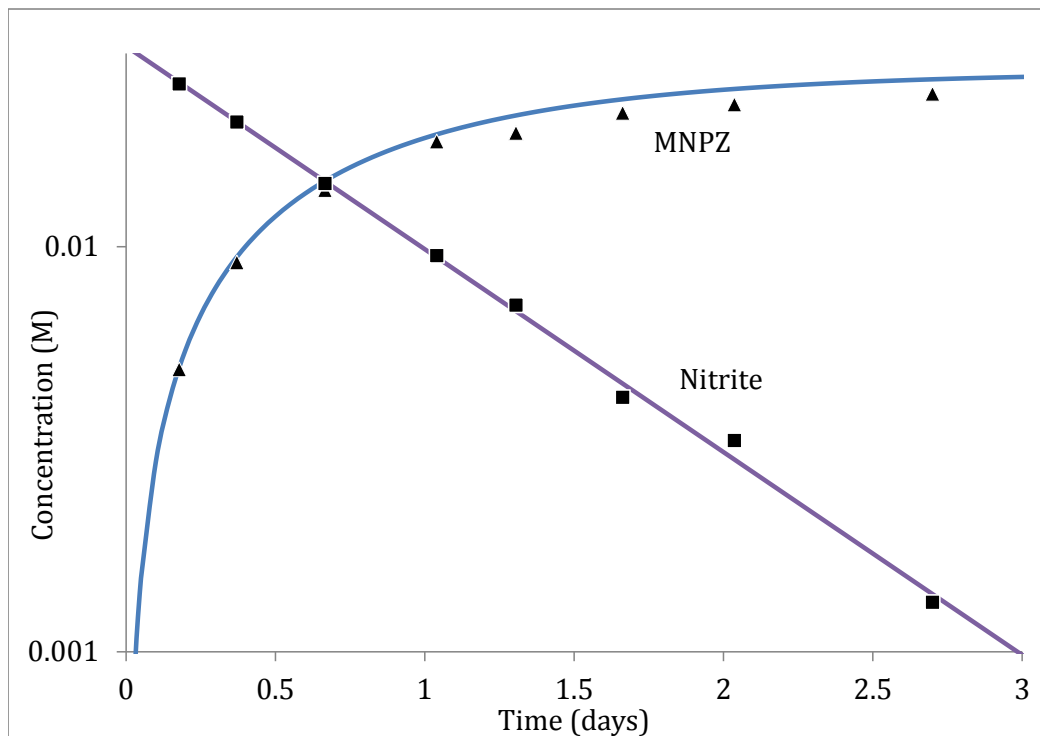


Figure 3.1: MNPZ formation in 5 M PZ loaded to 0.60 mol CO₂/mol PZ at 80°C. Curves calculated with $k_{obs} = 13 \times 10^{-6} \text{s}^{-1}$

3.1 Nitrite Dependence

MNPZ formation is first order in nitrite. Using a linear regression derived from Equation 2, the average coefficient of determination for all piperazine experiments is 0.991. Figure 3.1 shows this first order dependence by the apparent linear decrease of nitrite on a log scale.

The decrease in nitrite is associated with a stoichiometric increase in MNPZ. The curves were calculated from the equation in the figure using a rate constant, k_{obs} of $13 \times 10^{-6} \text{s}^{-1}$. The slightly lower calculated MNPZ con-

centration may result from MNPZ degradation, bias in the calibration curves, or a yield less than one.

$$\frac{dMNPZ}{dt} = k_{obs}[NO_2^-] \quad (3.1)$$

Using data similar to Figure 3.1, an observed first order rate constant, k_{obs} , was determined from the nitrite for 4 sets of reaction conditions. Experiments were conducted with 5 M PZ with between 0.2-0.8 mol CO₂/mol PZ, with between 0.5-5 M PZ and 0.6 mol CO₂/mol PZ, with 5 M PZ at lower temperature, and with 0.1 M PZ in a phosphate buffer.

3.2 pH Dependence

Four experiments with equal bicarbonate and PZ and with different proportions of monobasic and dibasic phosphate had a pH at room temperature between 7.1 and 7.8. The van't Hoff equation and thermodynamic data were used to estimate the pH at reaction conditions.[12, 1] The pK_a difference of a monobasic phosphate buffer between the oven conditions (135°C) and room temperature is 0.17. This difference would correspond to a similar change in pH for the four solutions because the solutions are in the range of the phosphate buffer.

The pH measurements at room temperature were adjusted to account for the increase in pK_a of the buffer at 135°C. Figure 3.3 demonstrates a first order dependence of k_{obs} on H⁺ concentration determined from the pH with a

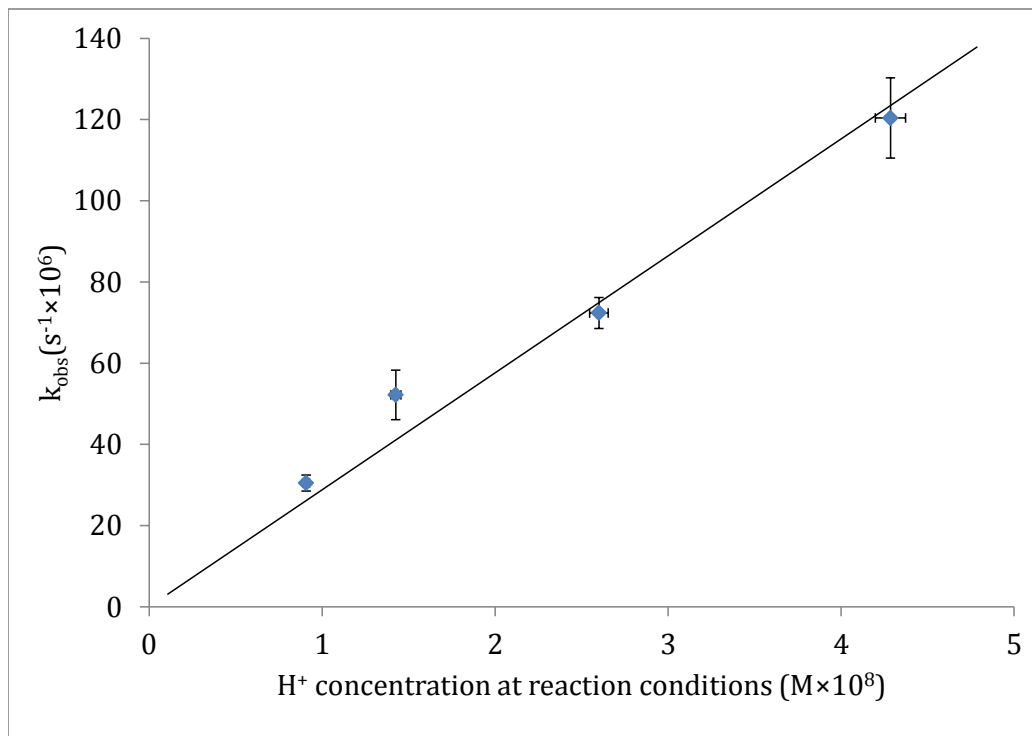


Figure 3.2: Varying pH in 0.5 M phosphate with 0.1 M PZ and a loading of 0.4 mol CO₂/mol PZ. The H⁺ concentration is given by the negative log of the pH.

coefficient of determination of 0.96.

From this analysis, the observed rate constants were normalized for pH at the reaction conditions by defining k_2 using the following equation:

$$\frac{dMNPZ}{dt} = k_2[NO_2^-][H^+] \quad (3.2)$$

The formation of nitrosamines, shown by Figure 1.6, indicates the production of a basic product. Solutions without a phosphate buffer would still

have a relatively stable pH because they contain two buffers: protonated and unprotonated amine as well as protonated and unprotonated amine carbamate. This natural buffering effect, along with the minimal concentration of nitrite added, significantly reduces the potential change in pH during nitrosation of the more concentrated amine solutions.

3.3 Carbamate Dependence

Previous work has suggested that CO_2 plays a role in nitrosation of CO_2 capture solvents. To test the effect of CO_2 , strong acid was added to match the pH of solutions with and without significant quantities of CO_2 . A 4.3 M PZ solution with 0.25 mol H_2SO_4 / mol PZ was heated to 100°C to determine how nitrosation occurs with low total CO_2 . The solution absorbed atmospheric CO_2 to a low loading of 0.002 mol CO_2 /mol PZ during solution preparation. The k_{obs} for this condition was $3.1 \times 10^6\text{s}^{-1}$. This rate is significantly slower than $112 \times 10^6\text{s}^{-1}$, the rate in 5 M PZ with a loading of 0.6 mol CO_2 /mol PZ heated to 100°C . Despite the large rate difference, the pH difference between the two experiments was only 0.12 ± 0.06 . Since the two solutions with different amounts of carbamate resulted in large reaction rate differences, total dissolved CO_2 significantly catalyzes nitrosation.

To understand how absorbed CO_2 affects nitrosation, the speciation of CO_2 inside PZ solution must be understood. All of the CO_2 added to the system can exist as physically absorbed CO_2 , bicarbonate, or as a carbamate with PZ. In our experiments, the majority of CO_2 exists as a carbamate. Since PZ

contains two secondary amines, a PZ carbamate molecule can either contain an unprotonated amine, a protonated amine, or a carbamate group on the other amine group. These species are called PZ carbamate, protonated PZ carbamate, and PZ dicarbamate, respectively. At high pH and low total dissolved CO₂, PZ carbamate dominates. As more CO₂ is added, the PZ carbamate concentration starts to decrease and protonated PZ carbamate and PZ dicarbamate concentrations increase. When the total dissolved CO₂ approaches the amount of PZ, significant bicarbonate concentrations arise, but this condition is not often seen in carbon capture systems with PZ. More information about speciation can be found in previous literature.[19, 9]

To discover which species containing CO₂ are reactive, the authors used the Independence thermodynamic model in Aspen Plus to calculate the pH and speciation of 7 solutions heated to 100°C.[10] From this, the k_2 for each set of solutions was determined from Equation 3.2. A rate constant, k_t , was defined to determine the species that catalyze nitrosation along with the order of concentration dependence.

$$k_t = \frac{k_2}{[C_{species}]^\alpha} \quad (3.3)$$

Table 3.2 lists each species analyzed in the 7 experiments at 100°C. For each species in Table 3.2, an order of reaction was found that resulted in the smallest relative standard deviation between the 7 experiments, representing the best correlation between reaction rate and the species concentration.

Table 3.2: Reaction dependence on different carbamate species. Total dissolved CO₂ represents all CO₂ added to the system. Relative standard deviation of k_t for 7 experiments found using Equation 3.3.

Carbamate Species	Optimized α	Relative standard deviation of k_t with optimized α	Relative standard deviation of k_t with $\alpha=1$
Physically Dissolved CO ₂	0.30	0.50	1.46
Bicarbonate	0.50	0.51	0.94
PZ carbamate	0.00	0.74	0.91
Protonated PZ carbamate	0.77	0.19	0.30
PZ dicarbamate	0.39	0.37	1.32
Total CO ₂ as carbamate	0.87	0.22	0.28
Total dissolved CO ₂	1.09	0.17	0.18

The high errors associated with the individual carbamate species is likely due to multiple carbamate species participating in nitrosation. Multiple PZ carbamate species can catalyze nitrosation as long as the two amine groups on PZ function semi-independently. Previous research indicates that protonation of the inactive nitrogen on PZ does not make the other nitrogen-containing group unreactive.[4] The ability for multiple carbamate groups to participate in reaction would explain why none of the individual carbamate species had both an order of reaction similar to stoichiometric orders of reaction (0.5, 1, 2) and a low relative error. The total carbamate species correlated better than any particular carbamate species because of this additive affect. Since the different carbamate species are likely to have slightly different rate constants, there is some error associated with using the sum of all carbamate species. However, uncertainties in the speciation model prohibit any meaningful analysis on the individual carbamate rate constants.

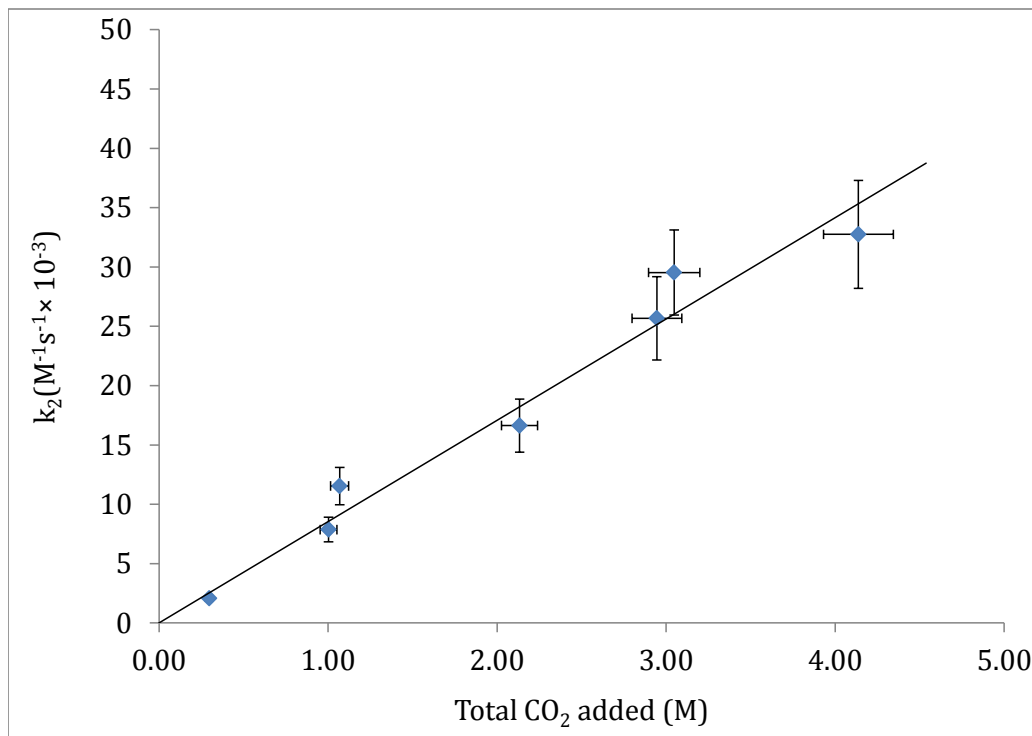


Figure 3.3: Reaction rate dependence on total dissolved CO₂ in 0.5, 1.7, and 5 M PZ with 0.6 mol CO₂/mol PZ and 5 M PZ with 0.1, 0.2, 0.3, 0.8 mol CO₂/mol PZ.

The total dissolved CO₂ is a practical way to determine total carbamate concentration in most solutions since physically dissolved CO₂ and bicarbonate are only present at low concentrations. Figure 3.3 demonstrates this practical correlation in experiments with 0.5 to 5 M PZ over a range of loadings.

Using the effect of carbamate, Equation 3.4 represents a simplified rate equation which agrees with the experimental data.

$$\frac{dMNPZ}{dt} = k_3[NO_2^-][H^+][R_2NCOO^-] \quad (3.4)$$

R_2NCOO^- corresponds to the carbamate species in the solution, but it is calculated using the total amount of CO_2 added per volume solution. As long as the moles of CO_2 are fewer than the moles of PZ, this approximation will hold. With more CO_2 than PZ, significant levels of bicarbonate form.

3.4 Temperature Dependence

Nitrosation is faster at higher temperature. Two effects cause this change: there is more thermal energy to overcome the activation energy, and the pH decreases with temperature due to the temperature dependence of the pK_a of PZ. After normalizing the rate constant for the pH and total CO_2 , the activation energy was determined to be 80 ± 2 kJ/mol (Figure 3.4).

3.5 Kinetic Model

Using the temperature dependence and Equation 3.4, a model for MNPZ formation can predict nitrosation of PZ by aqueous nitrite in the presence of CO_2 . All of the k_3 values, except the experiment with added sulfuric acid, were normalized to $100^\circ C$ and averaged to obtain the preexponential factor, $k_{3,avg} \approx 8.6 \times 10^3 \pm 1.1 \times 10^3 \text{ M}^{-2}\text{s}^{-1}$.

$$\frac{dMNPZ}{dt} = k_{3,avg} e^{\frac{E_a}{R} \left(\frac{1}{373K} - \frac{1}{T_{exp}} \right)} [NO_2^-][H^+][CO_2added] \quad (3.5)$$

The CO_2 loading should be less than 1.0 mol/mol PZ for this model to accurately predict kinetics. This model might not be applicable in the presence

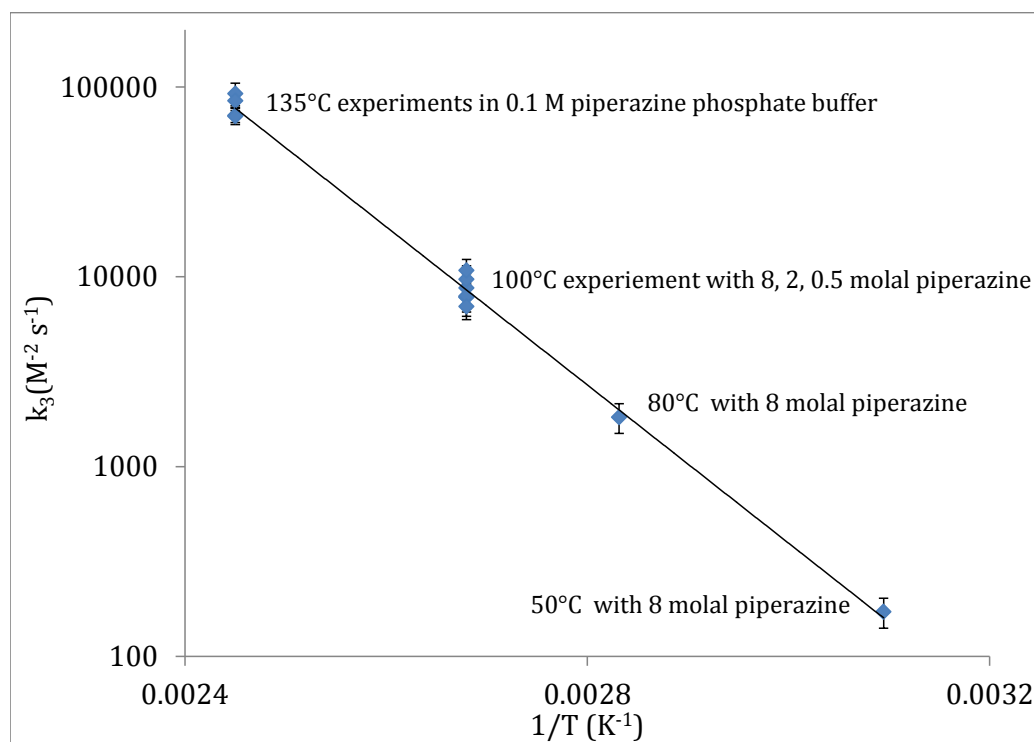


Figure 3.4: Reaction rate dependence on temperature for PZ. $E_a = 80 \pm 2$ kJ/mol.

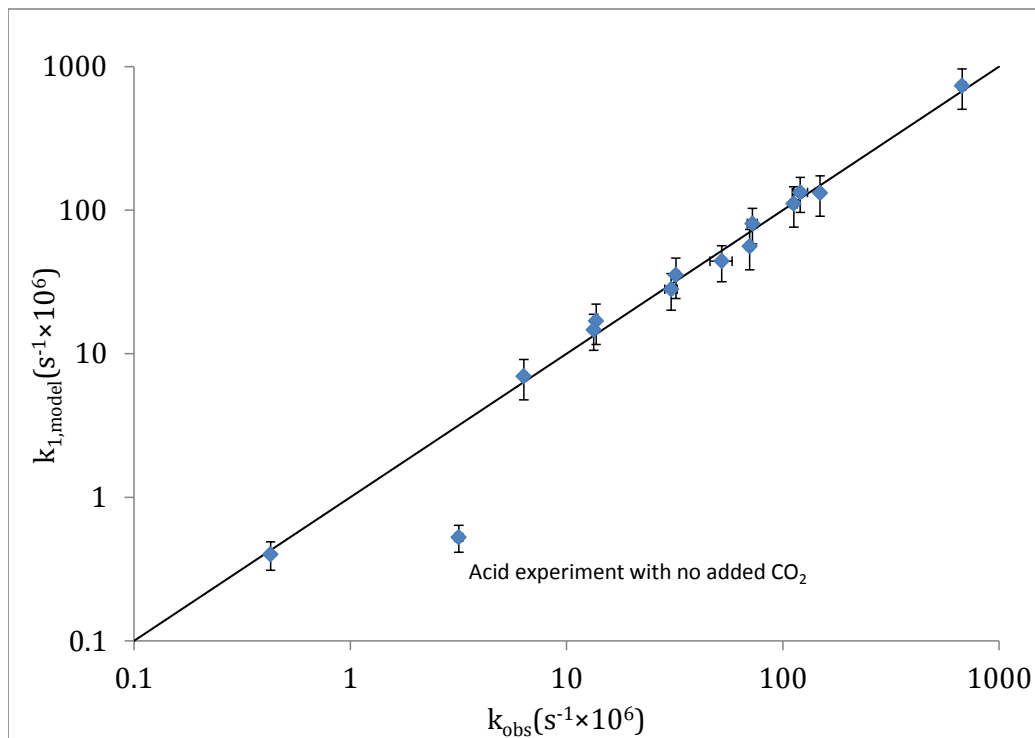


Figure 3.5: The $k_{1,model}$ for each experiment was obtained from the model using Equation 3.6. The line indicates perfect agreement between experimental and predicted data. The acid experiment was not regressed.

of significant amounts of formaldehyde which can also catalyze nitrosation at similar conditions as CO_2 .^[3] Previously published data on the pH of PZ can be used to determine the hydrogen ion concentration.^[10] Using Equation 3.1 and Equation 3.5, a predicted first order rate constant, $k_{1,model}$ was derived.

$$k_{1,model} = k_{3,avg} e^{\frac{E_a}{R} \left(\frac{1}{373K} - \frac{1}{T_{exp}} \right)} [H^+][CO_2 added] \quad (3.6)$$

Figure 3.5 shows how the observed first order rate constants, k_{obs} , com-

pare to predicted first order constants, $k_{1,model}$, from Equation 3.6. In this figure, the acid experiment with minimal CO₂ shows significantly higher rate than the model predicts. This indicates that at low carbamate concentrations, a different nitrosation reaction may dominate.

Chapter 4

Amine Comparison

This chapter expands on the model presented in chapter 3 by explaining and comparing the reaction kinetics of a primary, a tertiary, and various secondary amines. Two possible mechanisms are proposed followed by the overall thesis's significance and future directions.

4.1 Nitrite Consumption in Primary Amines

Experiments were conducted to see if MEA nitrosation kinetics were comparable to PZ. To accomplish this, four solutions were created at MEA concentrations of 7 and 3 molal with loadings of 0.2 and 0.4 mol CO₂/mol MEA. These solutions were heated between 100°C and 135°C.

After unloading the cylinders, a slight fizzing sound indicated that the cylinders increased in pressure from when they were loaded. This observation was followed by the formation of bubbles within the amber storage vials. These observations occurred because of N₂ formation from the decomposition of a primary nitrosamine as shown in Figure 1.7.

Since the MEA nitrosamines degraded during the reaction timespan, the reaction rate was determined by the disappearance of nitrite in the sam-

ple. This may lead to some inaccuracies in the reaction rate due to potential side reactions. However, the nitrite disappearance appeared clearly first order with a coefficient of determination of 0.997, and the presence of bubbles indicated that primary nitrosamines were a primary product, so the nitrite disappearance results are indicative nitrosation of MEA.

A first order rate constant, k_{obs} , was derived for nine experiments of MEA. This value was then regressed for the predicted pH at reaction conditions and the total amount of dissolved CO_2 . As done in section 3.5, all the experiments with MEA were regressed together. These experiments gave an activation energy of 81 ± 6 kJ/mol and preexponential constant of 560 ± 110 $M^{-2}s^{-1}$. The activation energy is comparable to PZ, but the preexponential constant is over $10\times$ smaller than PZ, so MEA will likely react with significantly less nitrite than PZ when mixed.

Since the nitrosamine formed by MEA decomposed significantly during the experimental runs, the amount of nitrite disappearance does not directly correlate with the amount of nitrosamine in the system. Equation 3.5 was generalized to remove the concentration of nitrosamine.

$$r = k_{3,avg} e^{\frac{E_a}{R} (\frac{1}{373K} - \frac{1}{T_{exp}})} [NO_2^-][H^+][CO_2added] \quad (4.1)$$

Figure 4.1 indicates an good fit between the model developed for PZ and the MEA reaction rates. This factor supports the notion that both PZ and MEA undergo a similar reaction mechanism.

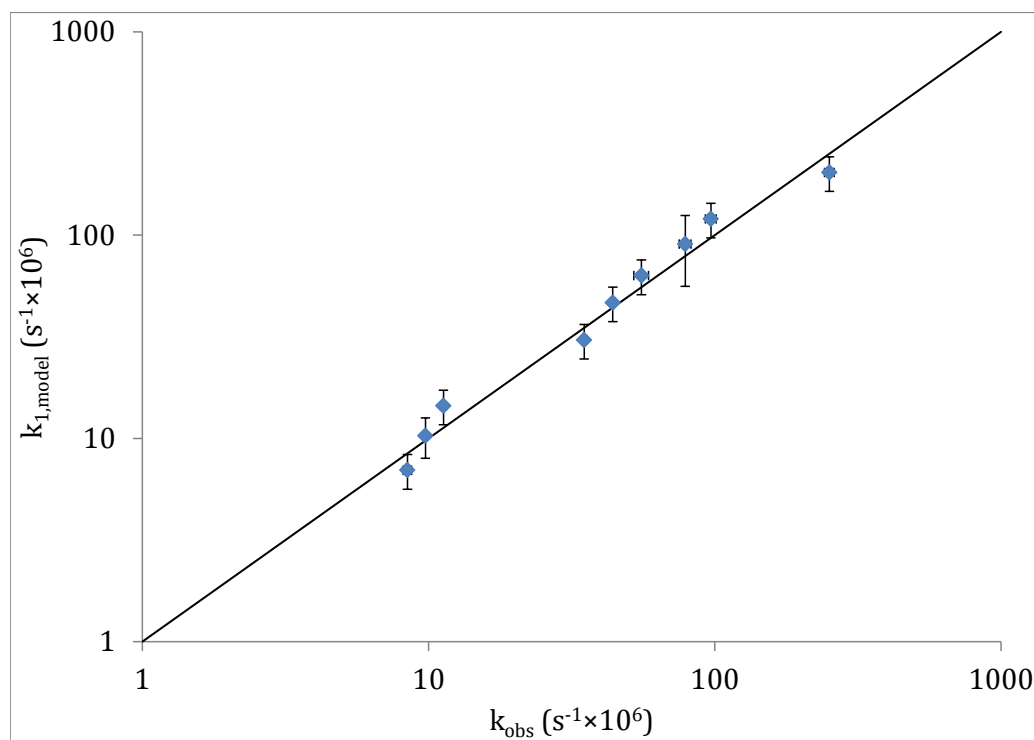


Figure 4.1: The predicted rate constant for MEA using Equation 3.6 and an activation energy of 81 kJ/mol correlates well with the experimentally observed rate constant.

4.2 Nitrosamine Formation in Tertiary Amines

As mentioned in subsection 1.5.3, tertiary amines are unable to form carbamate, so they likely undergo a different reaction mechanism than primary or secondary amines. To test if tertiary amines nitrosate using the same rate law, an experiment was conducted to see the affect of carbonate species while holding pH and temperature constant.

To obtain the reaction conditions required, a solution of MDEA (see Figure 1.5 for structure) and water at approximately 1.4 mol MDEA/kg solution was prepared. Potassium bicarbonate was then added to half of the solution to artificially alter the concentration of CO₂ species without a significant change in pH.

The solution with bicarbonate started forming a white salt after the addition of sodium nitrite at room temperature. The solution was decanted during the first four days after preparation. Salt formation decreased significantly over the 4 days and did not accumulate enough to form a complete layer on a 4 cm diameter vial. The salt composition likely involved sodium carbonate, but no composition analysis was conducted.

The pH after the salt formation of the bicarbonate and bicarbonate free solution were 8.878 and 8.882, respectively. Likewise, the amine concentration for both solutions 1.431 and 1.434 mol MDEA/kg solution respectively. Using total inorganic carbon analysis, the amount of carbamate species in the bicarbonate free solution was 0.0003 mol CO₂/mol MDEA while the solution

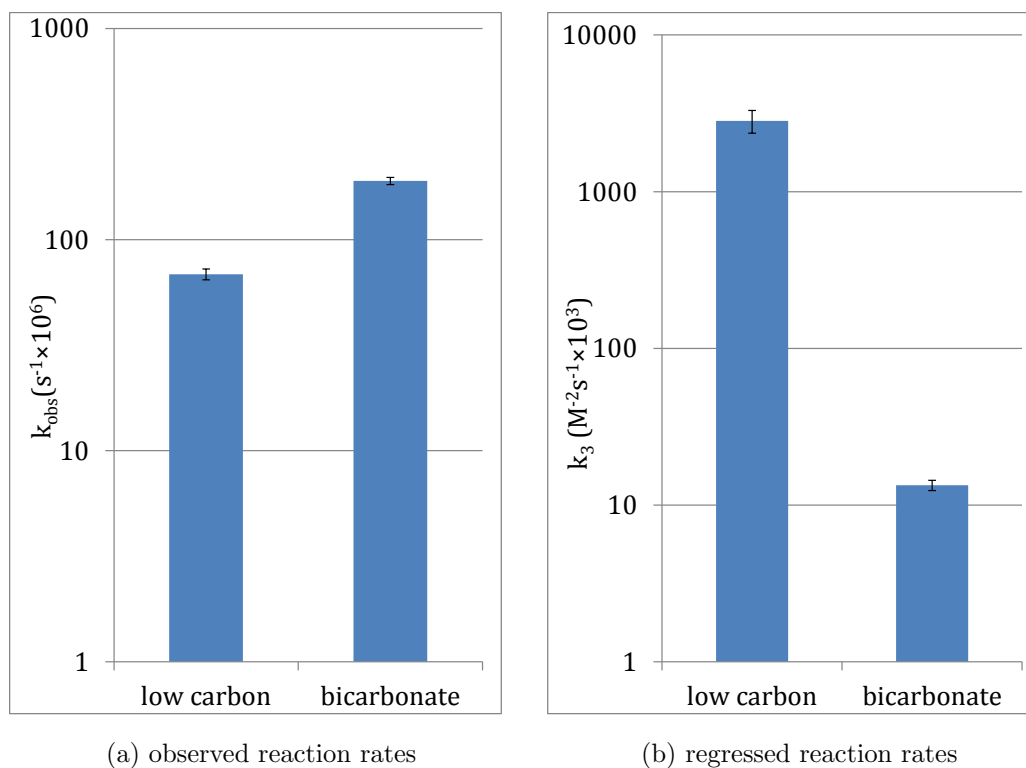


Figure 4.2: Rate constants of MDEA without CO₂ taken into account (left) and with regression for pH and inorganic carbon (right)

with bicarbonate had 0.16 mol CO₂/mol MDEA. The solutions were heated to 120°C for 6 hours. Figure 4.2 shows the observed reaction rates of both solutions with the third order rate constants, k_3 , similar to those for PZ and MEA analysis. The third order rate constant was found in a similar manner to PZ.

$$k_3 = \frac{k_{obs}}{[H^+][CO_2 species]} \quad (4.2)$$

Figure 4.2 shows that the k_{obs} of the bicarbonate loaded solution was three times the k_{obs} of the solution without bicarbonate added. This difference cannot be attributed to a catalytic affect of bicarbonate since the concentration of bicarbonate was over 500 times higher in the solution with added bicarbonate.

Two potential effects can explain the difference in k_{obs} . The less significant explanation involves the CO_2 species catalyzing nitrosation of secondary amine impurities within the solution. Due to safety concerns with nitrosamines, only enough nitrite to correspond with less than 2% nitrosation of amines is used. Since the purity on a mass basis of the MDEA used was rated as greater than 99%, there is a possibility that some nitrosation of secondary impurities increased the reaction rate. The nitrite disappearance had a coefficient of 0.995 indicating an acceptable first order fit, but a slightly steeper slope in the initial samples supports that impurities may have played an effect.

Another possible reason for the reaction rate difference involves the $\text{p}K_a$ shift of MDEA and bicarbonate with increasing temperatures. Since the solution was not buffered, the analysis explained in subsection 2.6.2 can not predict the pH. However, at reaction conditions the $\text{p}K_a$ of MDEA is 6.5 while the $\text{p}K_a$ of carbonic acid is 6.0.[16, 1, 2] In this situation, significant bicarbonate would be protonated to form carbonic acid and aqueous CO_2 . This reaction would leave more unprotonated MDEA, leading to a smaller drop in pH with temperature for the bicarbonate solution. This basic analysis

does not account for changes in activation energy which may result in a more acidic solution.

The differences in k_{obs} are insignificant when compared to the k_3 values shown in Figure 4.2. When normalizing for the amount of CO_2 in the solution, rate constants diverged for the two experiments, indicating that first order CO_2 does not fit MDEA. From these experiments, tertiary amines are not dependent of existence of carbonate compounds, so they fit a different rate law than secondary and primary amines amines.

Using a total nitrosamine analysis currently being developed, the nitrite disappearance in MDEA corresponds with nitrosamine formation. Further kinetic studies are necessary to understand which nitrosamine forms and the mechanism of formation. This analysis supports the use of nitrite disappearance to study amine reaction rate even for amines that do not nitrosate readily.

4.3 Nitrosamine Formation in Secondary Amines

To better understand the mechanism of nitrosation and to obtain useful data for other secondary amines in carbon capture, experimental tests similar to those in section 4.1 were conducted for both DEA and MMEA.

4.3.1 Diethanol Amine

Diethanol amine (DEA) is very similar to MEA; it just contains an extra ethanol substituent on the amine group. DEA was tested to both show

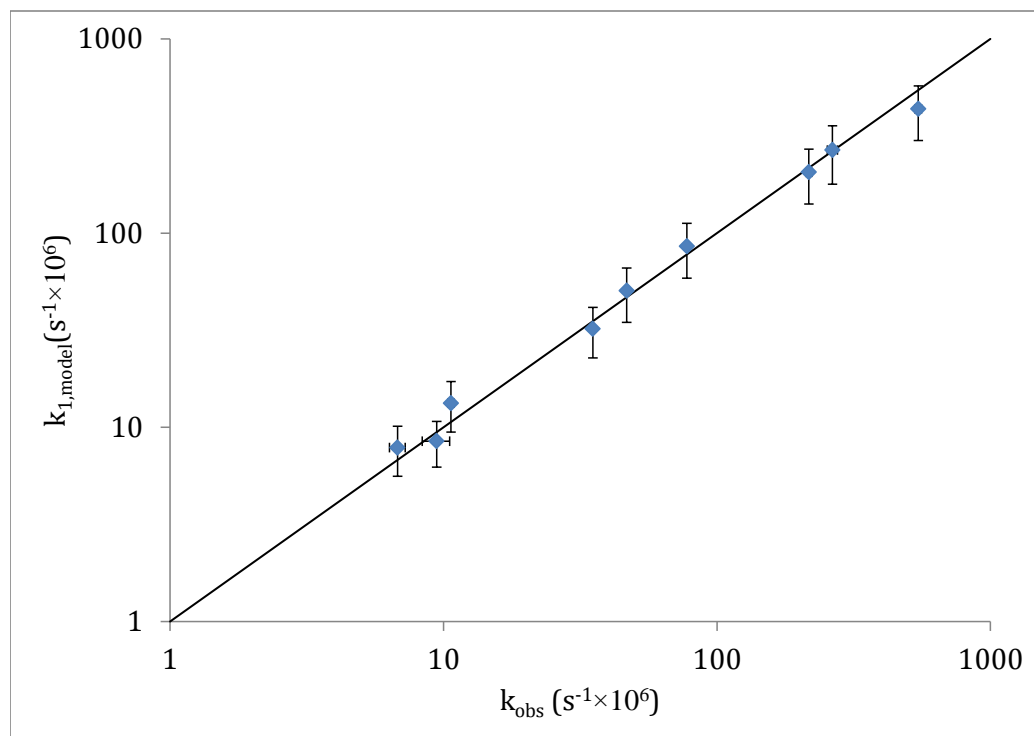


Figure 4.3: The predicted rate constant for DEA using Equation 3.6 and an activation energy of 60 kJ/mol correlates well with the experimentally observed rate constant.

the effect of the additional ethanol substituent and since DEA occurs in the production of MEA.

The experimental set for DEA included 9 experiments ranging from 3-7 molal DEA with 0.18-0.42 mol CO₂/mol DEA heated between 60-120°C. The k_{obs} for each set of conditions was normalized for pH and amount of CO₂. This data gave an activation energy of 60 ± 3 kJ/mol and a preexponential factor of $19 \times 10^3 \pm 3 \times 10^3$ M⁻²s⁻¹. This activation energy is about 25% less than E_a for PZ or MEA, and the $k_{3,avg}$ is significantly higher than both PZ and MEA.

Figure 4.3 shows a good correlation between the model and experimental rate. Comparing structure and reactivity is difficult between DEA and PZ because of the multiple differences in the molecular structures including cyclic or linear structures and presence of different electronegative groups.

4.3.2 Methylethanol Amine

To further clarify the structure property relationship in nitrosation of secondary amines, methylethanol amine (MMEA) was chosen since it replaces an ethanol group in DEA with a methyl group, reducing the electronegative pull of electrons from the nitrogen.

The experimental set for MMEA involved 8 experiments ranging from 1-5 molal MMEA with 0.19-0.38 mol CO₂/mol MMEA heated between 60-120°C. The k_{obs} for each set of conditions was normalized for pH and amount of CO₂.

This data gave an activation energy of 61 ± 4 kJ/mol and a preexponential factor of $16 \times 10^3 \pm 2 \times 10^3$ M⁻²s⁻¹. This activation energy and preexponential factor is comparable to the that of MMEA. This indicates that the methyl substituent does not change reaction kinetics significantly when compared to an ethanol group. The primary difference between the rate of formation between MMEA and DEA depends on the difference in pK_a between the two amines. However, when mixed in the same solution, the pH that each amine experiences would be identical.

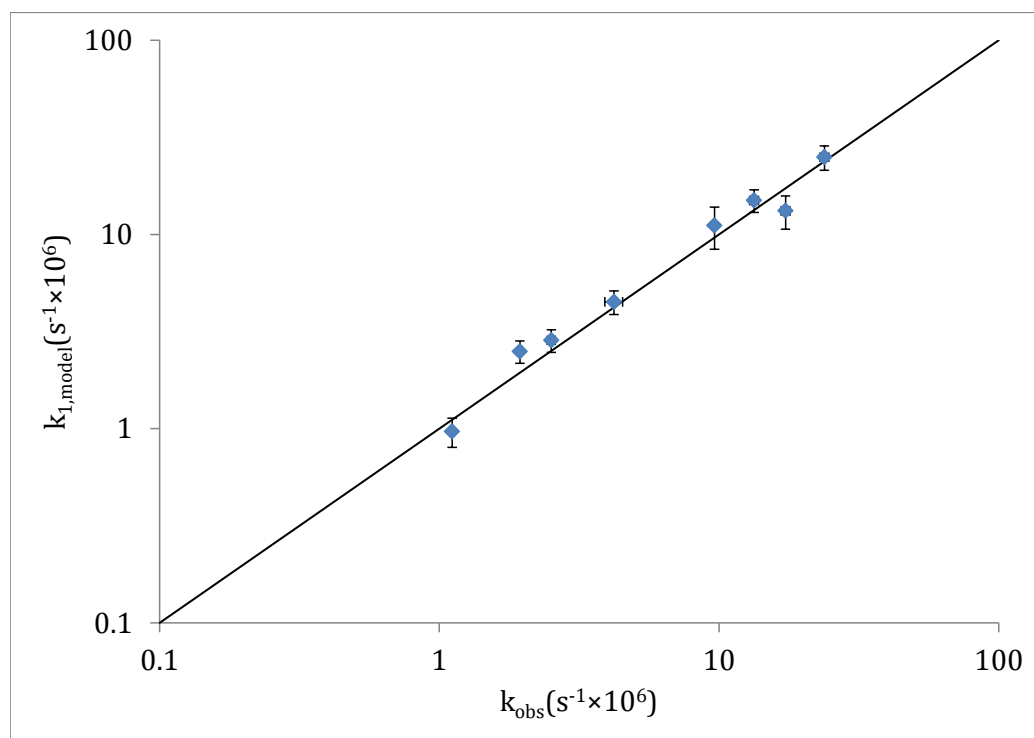


Figure 4.4: The predicted rate constant for MMEA using Equation 3.6 and an activation energy of 61 kJ/mol correlates well with the experimentally observed rate constant.

4.4 Rate Comparison

From the five amines studied, four accurately fit the model, so the rates of nitrosation of the various amines can be compared. By comparing the activation energy and reaction rate constants at 100°C, the effects of structure on reactivity can be determined. In addition, comparing amines at particular reaction conditions highlights the relative rates of nitrosamine formation of various amine solutions.

4.4.1 Activation Energy and Preexponential Factor

Figure 4.5 and Figure 4.6 compare the activation energy and average preexponential factor normalized to 100°C. The large similarity between DEA and MMEA indicates that the electronic withdrawing of the alkanols in DEA do increase reactivity (shown by the $k_{3,avg}$) but not significantly. PZ, as a cyclic molecule without alkanols, has a lower reactivity than both DEA and MMEA. The increased activation energy of PZ than the other secondary amines indicates some hindrance toward nitrosation potentially caused by steric effects of the cyclic structure.

4.4.2 Formation Rates at Conditions

Comparing the $k_{3,avg}$ is a poor indication of reaction rate since different amines give different solution pH and require different optimal loadings. The relative reaction rates shown in Figure 4.6 would apply best to amine blends since all the rates are normalized for pH. However, potential inaccuracies would

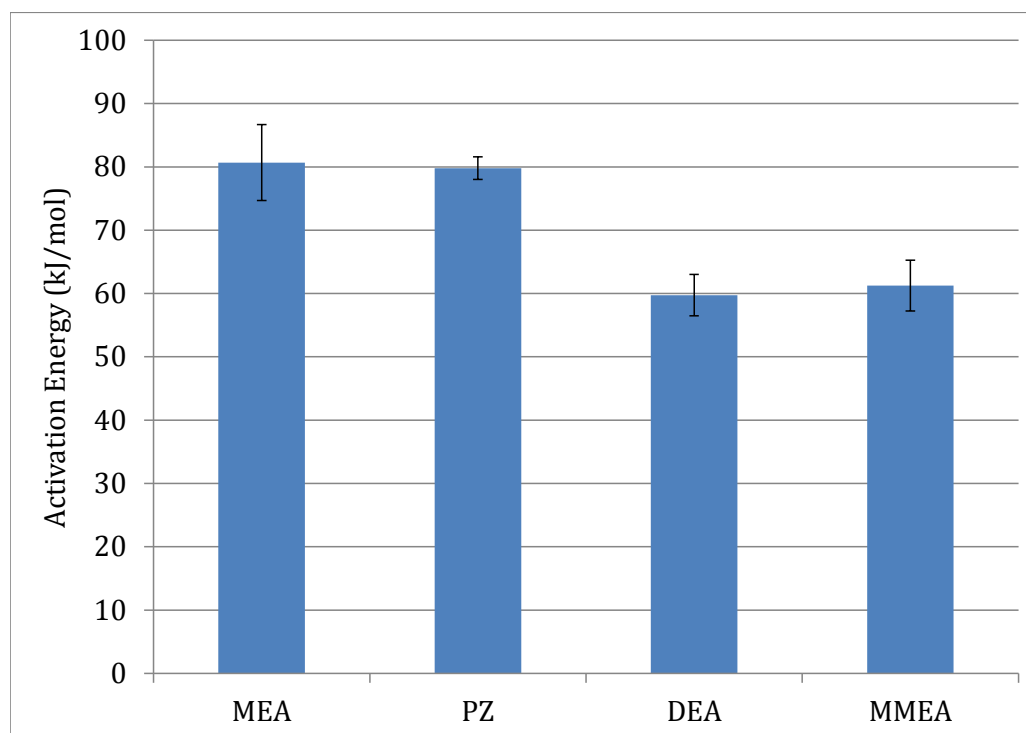


Figure 4.5: The activation energies for DEA and MMEA, two secondary alkanol amines, are 25% smaller than those of MEA, a primary amine, and PZ, a cyclic secondary diamine.

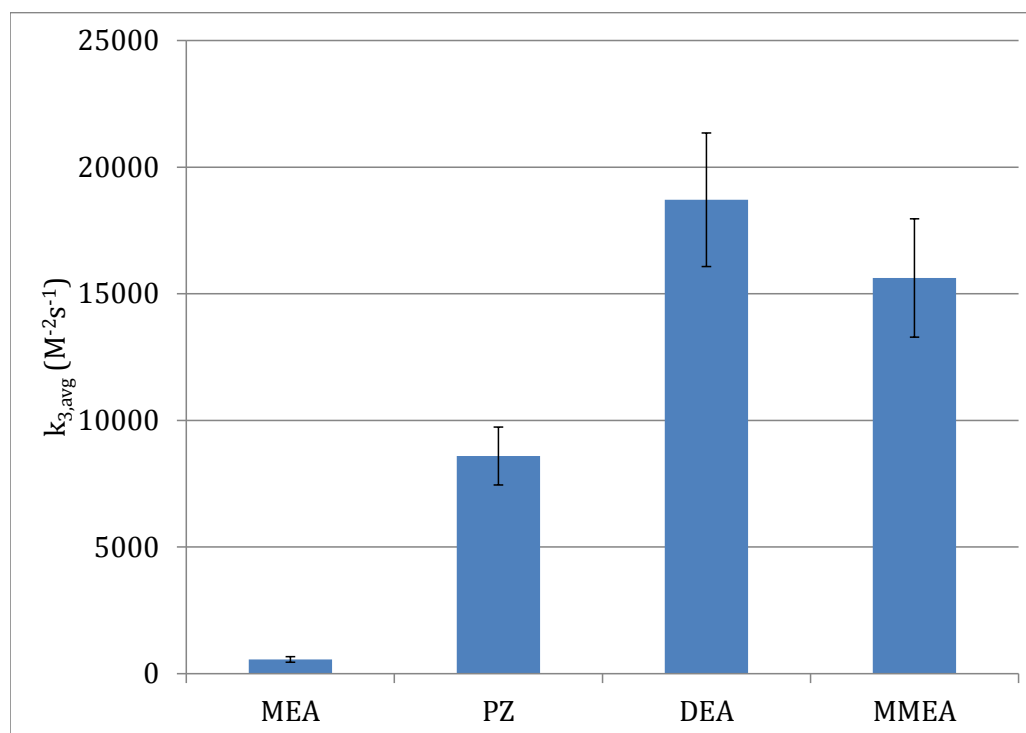


Figure 4.6: The preexponential factor normalized to 100°C, $k_{3,avg}$, for MEA, a primary amine, is significantly lower than the three secondary amines.

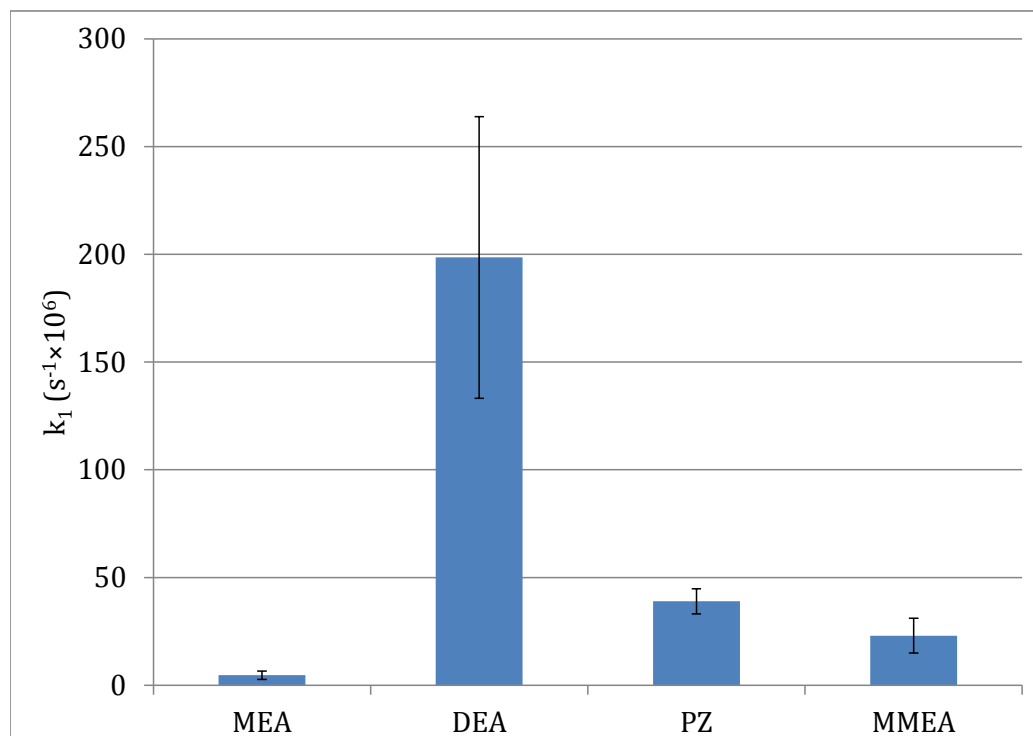


Figure 4.7: This graph shows the first order rate constants, k_1 , at 120°C for an amine concentration of 1.4 M loaded to 0.16 mol CO₂/mol amine group.

result from unequal formation of carbamate between different components.

Using predicted pH from subsection 2.6.3, the four amines were compared based on the pH they would produce at the same loading. Under these conditions, PZ holds twice the CO₂ than other amines since it has two amine groups. Figure 4.7 shows the first order reaction rate constants from this analysis. DEA shows a significant increase in reactivity when compared to the other amines since it has a low pK_a , so it produces a more acidic environment.

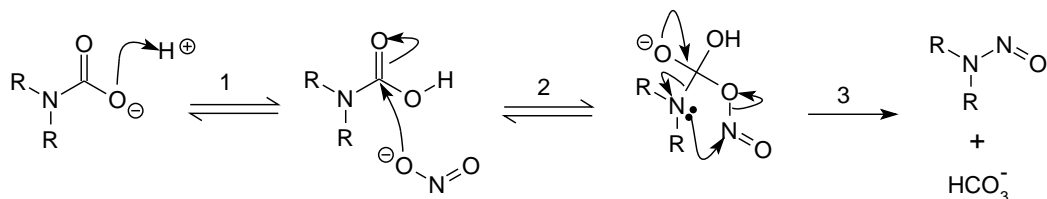


Figure 4.8: This mechanism is similar to that proposed by Lv and Sun.[22, 18]

4.5 Reaction Mechanism

Any valid reaction mechanism for unhindered primary and secondary amines must explain both the rate law and the increased reactivity of amines with less electron density. Two proposed mechanisms both include a nucleophilic attack of the carbamate carbon by nitrite, but differ in the degree of protonation and the number of steps required.

Figure 4.8 displays a mechanism which correlates with the experimental data. Step 1 is an equilibrium acid-base reaction. Since the $\text{p}K_a$ of the carbamate functional group is less than the pH of a typical solvent solution, the equilibrium would lie toward the unprotonated carbamate.[10, 5] Step 2 indicates a nucleophilic attack on the carbonyl group by the nitrite ion, and is the rate limiting step based on theoretical calculations.[22] This reaction would be easier the less electron density exists on the carbamate carbon. Step 3 includes the reformation of the carbonyl group accompanied by the formation of the N-nitrosamine bond in one concerted step.

Figure 4.9 shows an alternative mechanism that also explains experimental trends. The initial reactant shown is a protonated carbamic acid

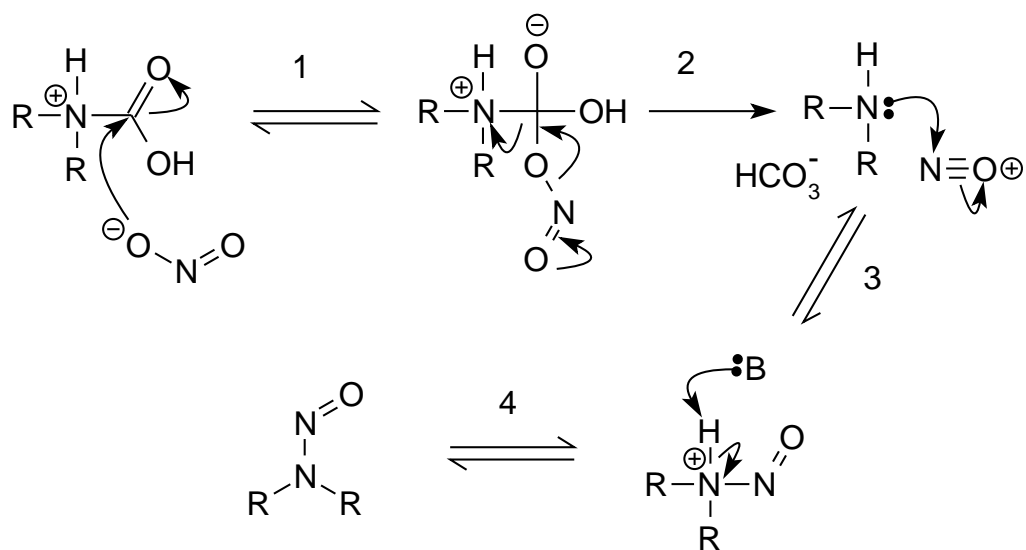


Figure 4.9: This mechanism includes an extra protonation to stabilize the negative charge, and it creates a nitrosonium ion intermediate similar to acidic reaction mechanisms.[7] Help with this mechanism was given by Dr. Eric V. Anslyn from the University of Texas at Austin

compound. This is favorable to balance the negative charge created from nitrite attachment. The first step involves the oxygen of nitrite attaching to the electrophilic carbamic acid. Just like the alternative mechanism, a greater reactivity would be achieved by having less electron density on the carbamic acid. The next two steps, 2 and 3, involve the formation of a nitrosonium ion and reattachment to the amine. The result from these steps is a protonated nitrosamine. These two steps essentially cover what occurs in step 3 in the previous mechanism. The final step involves the deprotonation of the nitrosamine to yield the product.

Both of these mechanisms show a first order dependence on hydrogen ions, carbamate, and nitrite while having increased reactivity as less electron density occurs around the carbamic acid. The differences highlight uncertainty as to how the reaction proceeds exactly.

4.6 Broader Impact

This research improved the understanding of nitrosamine formation in carbon capture by discovering a rate law, developing a model, and screening reactivity of various amines to discover reaction rates. The experiments confirmed that CO₂ catalyzes nitrosation for primary and secondary amines. The low reactivity of MEA, while still following the the secondary amine rate law, indicates a larger barrier to reactivity. The increased reactivity of amines with less electron density can help predict reactivity of other amines. Finally, the proposed mechanisms give a fundamental understanding to this reaction.

After understanding nitrosation, an emphasis on mitigating this reaction is necessary in carbon capture facilities. The formation of nitrosamines in carbon capture can be reduced through the use of nitrite scavengers or amine blends. Nitrite scavengers could prevent nitrosation, but most act through irreversible reactions. The scavenger products would accumulate in the solvent and lower the absorption performance. Using PZ blended with a primary or tertiary amine is another possibility to prevent nitrosamine formation because the primary amines do not form stable nitrosamines and tertiary amines resist nitrosation since an iminium ion is necessary.[7, 21] Significant work has already been conducted to study the performance of amine blends, but little research exists on the formation of nitrosamines in these blends.

The low reactivity of primary amines creates a challenge on mitigating nitrosamine formation. Using a blend which preferentially forms a carbamate with the primary amine could prevent the formation of stable nitrosamines, since nitrosamines from primary amines are unstable. Using the reactivities of PZ, MMEA, and DEA, the reactivities of other amines can be estimated based on the electron density of the amine functional group.

Another possible way to mitigate nitrosamine concentration is to cause denitrosation. Previous experiments indicate that nitrosamines thermally degrade at stripper temperature in carbon capture processes with no increase in equipment costs.[8] Another possibility for denitrosation includes UV degradation, though the opaque nature of degraded solvents would lower the efficiency of this method.[20]

In summary, nitrosation is a critical problem since it will hinder the application of amine scrubbing in carbon capture. Nitrite that forms from solvent absorption of NO_x will react with amines, especially at stripper conditions, to form nitrosamines. The kinetics for nitrosation in carbon capture conditions will be helpful when designing a system to minimize nitrosamine formation from nitrite. The various amines studied indicate the important factors of reactivity. Both mechanisms give a range of molecular reaction possibilities for the chemistry behind nitrosation in amine scrubbing.

Bibliography

- [1] P W Atkins and J de Paula. The response of equilibria to temperature. In *Physical Chemistry*, chapter 7.4. Oxford University Press, New York, 8 edition, 2006.
- [2] Robert L Berg and Cecil E Vanderzee. Thermodynamics of carbon dioxide and carbonic acid: (a) the standard enthalpies of solution of $\text{Na}_2\text{CO}_3(\text{s})$, $\text{NaHCO}_3(\text{s})$, and $\text{CO}_2(\text{g})$ in water at 298.15 K; (b) the standard enthalpies of formation, standard Gibbs energies of formation, and standard entropies of. *The Journal of Chemical Thermodynamics*, 10(12):1113–1136, December 1978.
- [3] Julia Casado, Manuel Mosquera, Carlos Paz, Flor Rodriguez-Prieto, and Jose Vázquez-Tat. Nitrite Ion as a Nitrosating Reagent. Nitrosation of Morpholine and Diethylamine in the Presence of Formaldehyde. *Journal of the Chemical Society. Perkin transactions 2*, (12):1963–1966, 1984.
- [4] Enrique A Castro, Andrea Hormazabal, and Jose G Santos. Concerted Mechanism of 4-Cyanobenzoate with Secondary Alicyclic Amines in Aqueous Ethanol. *International journal of chemical kinetics*, 30(4):267–272, 1997.
- [5] Chemical Abstracts Service. Scifinder Scholar, 2012.

- [6] Ning Dai, Amisha D Shah, Lanhua Hu, Michael J Plewa, Bruce Mckague, and William A Mitch. Measurement of Nitrosamine and Nitramine Formation from NO. *Environmental science & technology*, 46(17):9793–9801, 2012.
- [7] ML Douglass and BL Kabacoff. The chemistry of nitrosamine formation, inhibition and destruction. *Journal of the Society of Cosmetic Chemists*, 29(September):581–606, 1978.
- [8] Nathan Fine, Mark J Goldman, Paul T Nielsen, and Gary T Rochelle. Managing n-nitrosopiperazine and dinitrosopiperazine. *Energy procedia*, 2013.
- [9] Peter Frailie, Jorge Plaza, David Van Wagener, and Gary T. Rochelle. Modeling piperazine thermodynamics. *Energy procedia*, 4:35–42, January 2011.
- [10] Peter Frailie and Gary T Rochelle. Aspen Plus Independence Model, 2012.
- [11] Stephanie Anne Freeman. *Thermal Degradation and Oxidation of Aqueous Piperazine for Carbon Dioxide Capture*. Phd. dissertation, The University of Texas at Austin, 2011.
- [12] Robert N Goldberg, Nand Kishore, and Rebecca M Lennen. Thermodynamic Quantities for the Ionization Reactions of Buffers. *Journal of physical and chemical reference data*, 31(2):231–370, 2002.

- [13] Mark J Goldman, Nathan A Fine, and Gary T Rochelle. Kinetics of N-Nitrosopiperazine Formation from Nitrite and Piperazine in CO₂ Capture. *Environmental science & technology*, 47(7):3528–34, April 2013.
- [14] Espen S Hamborg and Geert F Versteeg. Dissociation Constants and Thermodynamic Properties of Amines and Alkanolamines from (293 to 353) K. *Journal of chemical engineering data*, 54:1318–1328, 2009.
- [15] Phil Jackson and Moetaz I Attalla. N-Nitrosopiperazines form at high pH in post-combustion capture solutions containing piperazine: a low-energy collisional behaviour study. *Rapid communications in mass spectrometry*, 24:3567–3577, 2010.
- [16] Inna Kim, Christian M. Jens, Andreas Grimstvedt, and Hallvard F. Svendsen. Thermodynamics of protonation of amines in aqueous solutions at elevated temperatures. *The Journal of Chemical Thermodynamics*, 43(11):1754–1762, November 2011.
- [17] Chun-Lin Lv, Yong Dong Liu, and Ru-Gang Zhong. Theoretical investigation of N-nitrosodimethylamine formation from dimethylamine nitrosation catalyzed by carbonyl compounds. *The journal of physical chemistry. A*, 113(4):713–8, January 2009.
- [18] Chun Lin Lv, Yong Dong Liu, Rugang Zhong, and Yunhai Wang. Theoretical studies on the formation of N-nitrosodimethylamine. *Journal of molecular structure. Theochem*, 802(1-3):1–6, January 2007.

- [19] Gary Rochelle, Eric Chen, Stephanie Freeman, David Van Wagener, Qing Xu, and Alexander Voice. Aqueous piperazine as the new standard for CO₂ capture technology. *Chemical engineering journal*, 171(3):725–733, July 2011.
- [20] Mihaela I. Stefan and James R. Bolton. UV direct photolysis of N-nitrosodimethylamine (NDMA): kinetic and product study. *Helvetica chimica acta*, 85(5):1416, May 2002.
- [21] Zhi Sun, Yong Dong Liu, and Ru Gang Zhong. Theoretical investigation of N-nitrosodimethylamine formation from nitrosation of trimethylamine. *The journal of physical chemistry. A*, 114(1):455–65, January 2010.
- [22] Zhi Sun, Yong Dong Liu, and Ru Gang Zhong. Carbon dioxide in the nitrosation of amine: catalyst or inhibitor? *The journal of physical chemistry. A*, 115(26):7753–64, July 2011.

Vita

Mark Jacob Goldman was born in El Paso, Texas during a frigid night in December 1991. He spent his first two years of life in his birth city with his immediate and extended family before moving to Sugar Land, Texas. There he attended Clements High School and was actively involved in Academic Decathlon, the environmental organization, and a competitive programming team. These activities highlight three of his passions: learning about the world, conserving natural resources, and solving challenging problems. He is currently working on his undergraduate degree at The University of Texas at Austin. His research on carcinogen formation in carbon capture with the Rochelle Group in Austin highlights all three of his passions. He plans to complete his degree in May 2014 after studying in Singapore. Then he aspires to enroll in a Ph.D. program in chemical engineering with a focus on sustainability.

Permanent address: 3314 Larkwood Lane
Sugar Land, Texas 77479